university of groningen / faculty of science and engineering

Design of an experiment to seal a submarine to the Ocean Battery shaft safely

Industrial engineering and management bachelor integration project

Author: Stijn Kram | S3371816

First supervisor:
Prof. Dr. A. Vakis
Second supervisor:
Msc. M. Mohebbi
Daily supervisor:
Drs. W. Prins

This page is intentionally left blank.

1 Abstract

A marine underwater energy storage system operates fully when engineers are able to enter the powerhouse to do maintenance on hydro turbines. A submarine must be designed to connect to the energy storage system to transfer people safely. However, the energy storage system is exposed to biofouling which causes high surface roughness over time. The increasing surface roughness has a negative effect on connecting and sealing the underwater energy storage system. The seals are made of rubber and the underwater energy storage system is made of steel on which barnacles and sponges will grow. For perfect alignment and sealing, the barnacles and sponges need to be removed leaving a lower surface roughness. In this study, experiments are taken to investigate the working principle of sealing rough surfaces and to simulate hydrostatic pressures at a depth ranging from 30 to 50 meters. Three different rubber O-ring seals are used and sandpaper is used for replicating the surface roughness. The surface roughness after removing biofouling is found and its effect on different seals. Additionally, the squeezing pressure on the seal is found needed to achieve an acceptable leakage rate.

Key words: energy storage system, submarine, diving bell, biofouling, sealing, seals, leakage rate, experiment, 3D optical profilometer, rubber

Table of contents

List of figures

List of tables

Abbreviations

Energy Storage Systems	ESS
Ocean battery	OB
Submarine rescue vehicle	SRV
Disabled submarine	DISSUB

2 Introduction

Currently, Energy Storage Systems (ESS) are of significant importance (AB Gallo, et al., 2016). Since ESS balances the supply and demand on the grid and it can help to support the integration of renewable energy sources into the grid. Renewable energy sources, such as solar and wind, are often intermittent and can be difficult to predict. ESS can help to smooth out the output of these sources and make them more viable as a source of electricity.

The Ocean Grazer BV is a company that stores and generates sustainable energy using innovative techniques in the ocean. At the beginning of 2022, the company won a prize in the category Innovation, Sustainability, Eco-design & Smart Energy (CES Innovation Awards, 2022). They won the prize with their innovative solution for ESS: the Ocean Battery (OB). This is an ESS that does not depend on scarce materials such as lithium.

To let the OB fully operate, engineers must be able to enter the powerhouse of the OB safely for maintenance. This powerhouse is located at the bottom of the OB and includes the hydro turbines. It can be entered by designing a submarine that can transport people from the submarine into the OB without becoming wet. For this, a docking mechanism should be designed to dock at the OB.

Submarine rescue vehicles (SRV) have proven this technology of transporting people underwater since 1939. NATO is continuously improving SRVs to rescue submarines worldwide faster and safer. (Nick Stewart, 2008)

At the left of figure 2.1, the cockpit is shown, in which the pilot will steer the SRV to the submarine. At the bottom of the SRV the docking mechanism is shown (or dry mating skirt), this part will connect to the disabled submarine (DISSUB). The pilot can maneuver the vehicle at the submarine's escape hatch with the use of cameras and sensors. When connected, the docking mechanism will drain the water out, causing a pressure difference and mutual suction of both vehicles.

Figure 2.1: The LR11, one of the newest submarine rescue vehicles (Richard S., 2021)

Although there seems to be a potential solution for entering the OB, there will be significant differences between entering a DISSUB or entering the OB. The SRV should first localize the DISSUB and should be able to dock at different angles. Contrary, the location of the OB is known and the docking surface will be parallel to the water surface. Another difference is that submarines are continuously moving and can be hoisted out of the water for cleaning. The OB is not moving during operation and is continuously submerged. As a result, significantly more biofouling will grow on the OB. Biofouling is the accumulation of sea organisms ranging from microorganisms to small animals where it is not wanted on underwater structures. The process of biofouling starts minutes after submersion, as minerals including proteins and polysaccharides, naturally dissolved in seawater, adhere to submerged structures. (Vinagre et al., 2020) The biofouling will deteriorate the surface through corrosion and shells. Additionally, sponges will increase the roughness of the substrate (Canning, 2020).

The seal of the docking mechanism is one of the most important components. The purpose of the seal is to prevent or reduce the leakage of fluid from one chamber to another. (Andrei et al., (2021) Most surfaces of engineering interest have surface roughness on a wide range of length scales (Persson, 2005), (from cm to nm) which will influence the leak rate and friction of seals,

and account for the whole range of the surface roughness is impossible using standard numerical methods, such as the Finite Element Method. (Lorenz et al., 2009)

It is found that the recommended maximum for sealing surfaces is 0.8 μm Ra. Mathematically, Ra is the arithmetic average value of the profile departure from the mean line, within a sampling length. (Robert F. , 2015) Therefore, the growth of biofouling should be removed to be able to seal the OB safely. This thesis aims to understand what impacts biofouling has on sealing a submarine to the OB.

The document will be structured in the following way: first, the introduction of the OB and docking at the OB. The literature review will elaborate on the phenomena of biofouling and (its effect on) sealing. Then the problem analysis includes the problem context, system description, stakeholder analysis, conceptual model, Problem statement, and research objective. The Research design will explain the research questions, the methods, the tools, the deliverables and, the validation of the project. Later on, the experiment will be conducted and the results will be analyzed. Moreover, future research is suggested to extend this project.

2.1 Ocean Battery

The mechanism of the OB is based on hydro dam technology that has proven itself for over a century as highly reliable and efficient. The design of the OB is depicted in figure 2.2. As can be seen in the figure, the OB consists of a rigid underwater reservoir, the shaft, and the flexible bladders. To store energy, the system pumps water from the rigid reservoirs into the flexible bladders on the seabed. Now the energy is stored as potential energy in the form of water under high pressure. When there is a demand for power, water flows back from the flexible bladders to the low pressure rigid reservoirs. This water flow drives multiple hydro turbines generating electricity. It can be deployed in existing and new offshore wind farms. It is located near the source, at the bottom of the ocean. It reduces peak loads and optimally coordinates the supply and demands of energy. (Ocean Grazer BV, 2022)

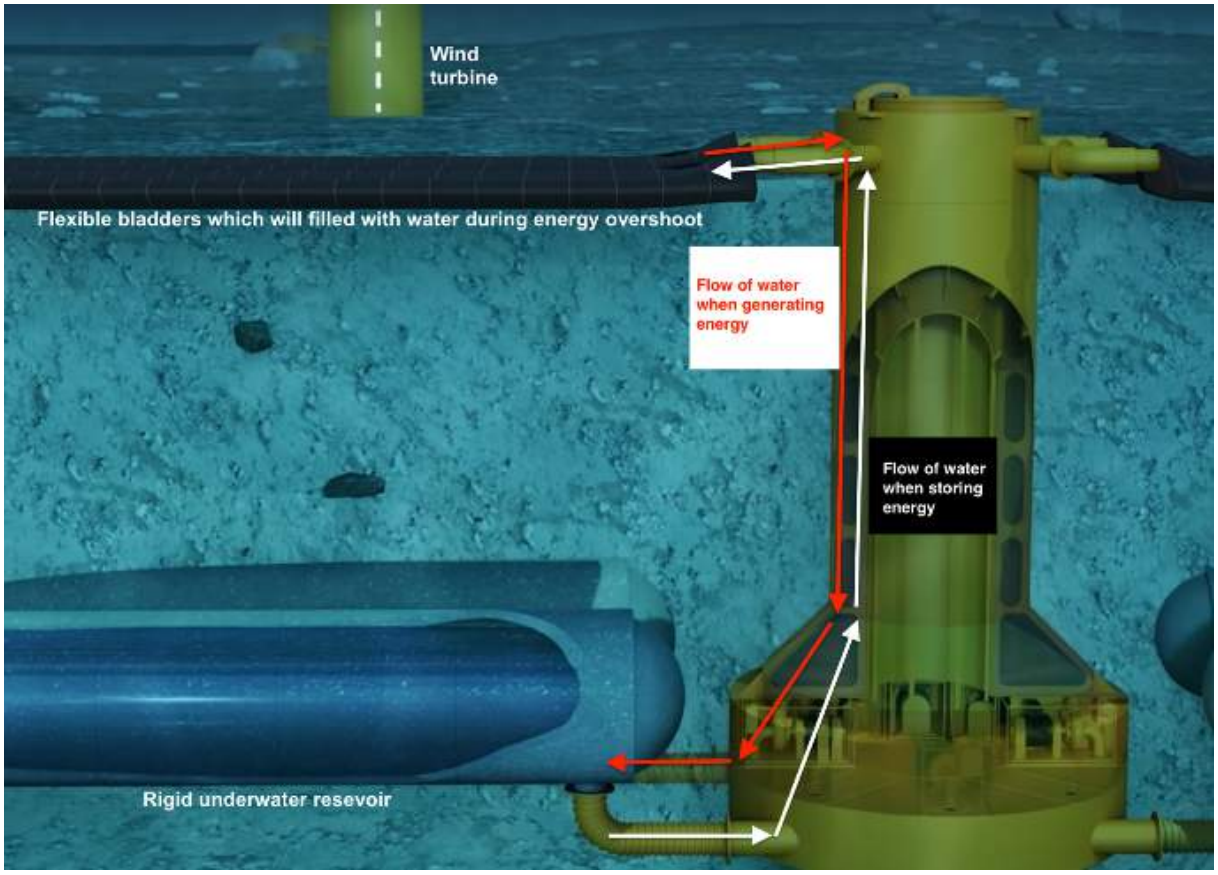

Figure 2.2: Schematic overview of how the Ocean Battery stores energy (Ocean Grazer BV., 2022)

2.2 Docking at the Ocean Battery

To let the OB fully operate, engineers must be able to enter the powerhouse of the OB safely for maintenance. This powerhouse is located at the bottom of the OB and includes the hydro turbines. It can be entered by designing a submarine that can transport people from the submarine into the OB without becoming wet. For this, a docking mechanism should be designed to dock at the OB.

The depth of the OB will range from 30 to 50 meters deep. The diameter of the shaft of the OB is 10 meters and it reaches from 1 meter above the seabed to 30 meters below. The pressure inside the submarine and the shaft are both 1 atmosphere.

Two processes of the docking mechanism should be considered: One mechanism for the transportation of only two crew members (and small tools). And one mechanism for crew and larger components such as pumps and turbines.

Additionally, the submarine will consist of a pressure cabin that can withstand the pressures at the given depths and the docking mechanism which is filled with water during descent. When looking at figure 2.3, it can be seen that the docking mechanism connects to the shaft (A). The O-ring, functioning as a seal, connects the two objects. A certain pressure P0 is needed on the seal to be able to drain the water out (B). If the P0 is high enough for the seal to reach an acceptable leakage rate, the water could completely be drained away. When the pressure inside the docking mechanism is regulated at 1 atm the hatch of the shaft could be opened. The drain causes a pressure difference of 2-4 atm and a mutual suction of the submarine and the shaft (C).

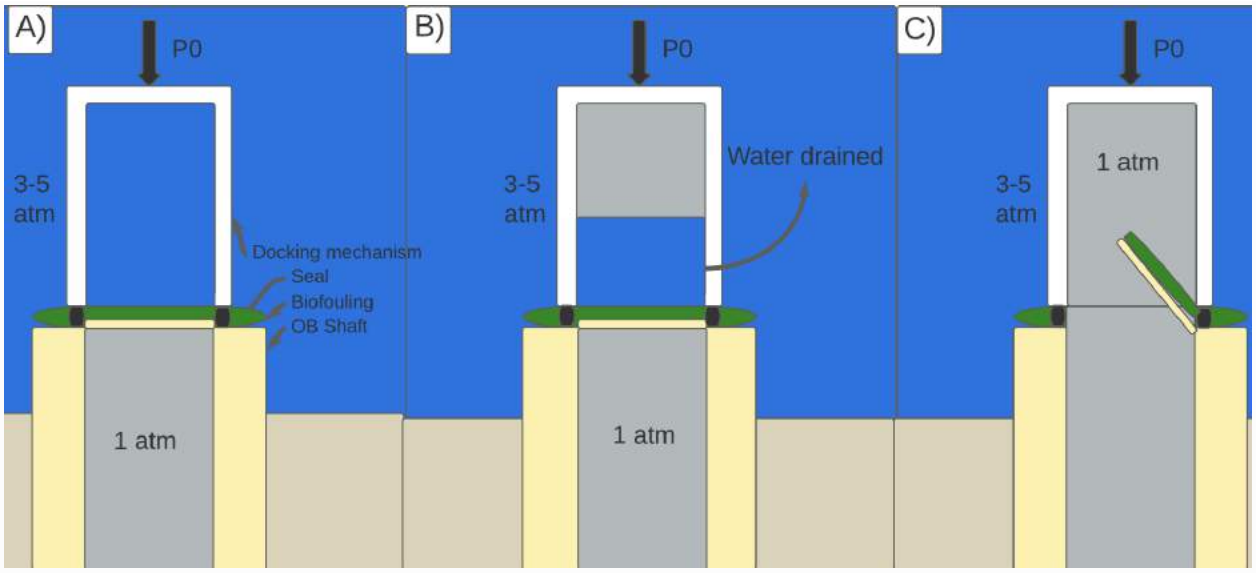

Figure 2.3: The steps of docking at the OB. Step A) is the first connection between the submarine and the OB shaft. A certain pressure P0 is needed in Step B) to drain the water out. When the pressure between the submarine and the shaft is equalized, the hatch can be opened C).

The sealing in steps B) and C) should control the desired leakage rate to drain the compartment successfully. This leakage rate can be obtained by manipulating the squeezing pressure, the surface roughness (or the biofilm), and the dimensions and characteristics of the O-ring seal. These factors will be explained in the following section.

3 Problem context

This section will elaborate on what biofouling is and how it grows. Furthermore, the section will elaborate on the principle of sealing and surface roughness.

3.1 Biofouling

Biofouling is the accumulation of sea organisms ranging from microorganisms to small animals where it is not wanted on underwater structures. The process of biofouling starts minutes after submersion, as minerals including proteins and polysaccharides naturally dissolved in the seawater adhere to submerged structures (Vinagre et al., 2020)
There are three stages of biofouling, the pioneer stage (0-2 years), the intermediate stage (3-5 years), and the climax stage (more than 6 years). Figure 3.1 shows different stages of biofouling growth. (Canning, 2020)

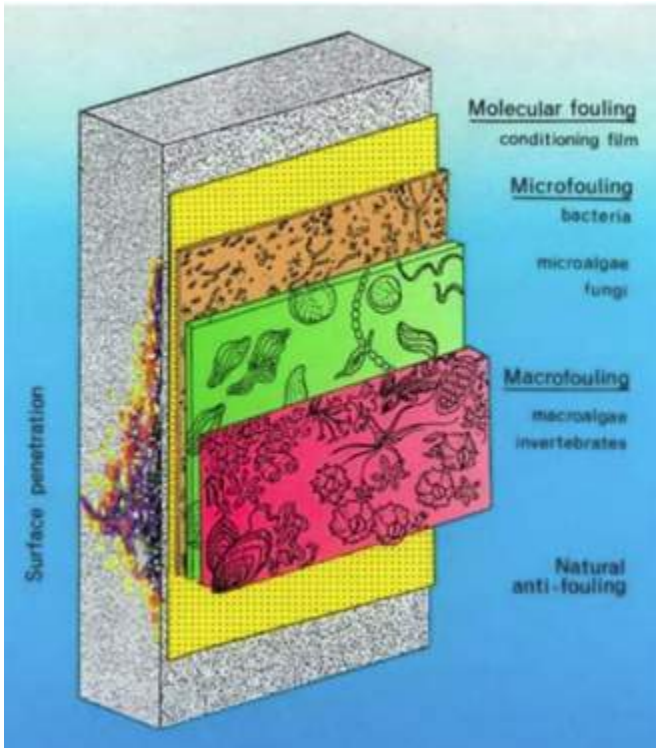

Figure 3.1: Different stages of biofouling. 1) Natural anti-fouling, 2) Molecular fouling 3) Microfouling, 4) Macrofouling and surface penetration. (Canning, 2020)

The growth of the biofilm is dependent on some external factors including seawater temperature, depth, light availability, currents, and distance to shore, topography and wettability of the substrate, material of substrate, and color of substrate. (Vinagre et al., 2020)
Additionally, the state that salinity, conductivity, pH, and dissolved oxygen content of seawater are other external factors influencing biofouling, as well as organisms already on the strata and the adhesion strength of organisms. (Kyei, S et al., 2020)

The effect of biofouling on the material is called biodeterioration. Five forms of deterioration will be elaborated on below:

- Microbiologically induced corrosion (MIC): Below the grown biofouling oxygen-depleted zones are created where corrosion processes thrive. And corrosion can cause pits and cracks in steel. (Canning, 2020)
- Biotic and Abiotic Degradation: biotic is breaking down molecules by enzymes. (ChemPro, 2016) And it proceeds via surface attack by bacteria present in the biofilm. (Gu, 2005). Examples of abiotic are oxidation and hydrolysis
- Micro Deterioration: Damage to the polymer chains inside the material may be caused due to swelling and bursting of growing cells of the microorganisms inside the material. (Rutkowska, M., et al. (2002)
- Abrasion & increased MIC: The forces of waves and currents on macro-organisms adhered to submerged structures cause abrasion due to the macro-organisms' adhesion strength in combination with their weight and volume (Vinagre et al., 2020) Furthermore, macrofouling increases corrosion as it induces oxygen-depleted zones (Kyei et al., 2020)
- Direct deterioration: Macro organisms that settle on the object can be destructive as they deteriorate the material by making holes and pits. (Jeroen Franssen, 2022)

Table 3.1 shows an overview of the different kinds of deterioration and its depth, distance to shore, location, and material on which it grows.

Table 3.1: Macro Organisms that induce direct deterioration of their habitat and deterioration information (Jeroen Franssen, 2022)

	Depth(m)	**Dis.to shore(km)**	**Location**	**Deterioration (mm/year)**	**Material**
Sponges	20-50	<50	West Scotland	-	-
Oysters	1-8	<50	Holland, Denmark	2	Steel
Mussels	<30	<50	all over	-	-
Martesia	all	all	no	see figure 3.7	PVC, HDPE
Teredines	all	all	-	-	Plastics
Barnacles	all	all	yes	2.5	Steel

For the interest of this research, it is important to know the dimensions and the material characteristics of the biofouling types occurring at a depth of 30 to 50 meters on steel. These will be sponges and barnacles.
From table 3.1 it can be seen that barnacles can cause pits of 2,5 mm per year.
The size of barnacles varies between 1,27 cm and 3,81 cm in height and between 1 cm and 7 cm in length. (AZanimals 2022)

3.2 Sealing

The technique of sealing is employed to prevent or reduce the leakage of fluid between different chambers through the utilization of seals. There are various types of seals that are commonly utilized, including face seals (gasket), O-ring seals, and labyrinth seals (Andrei et al., 2021). Among these, a surface-to-surface contact static seal is widely applied in several industries, including deep space exploration and nuclear power generation, and has been an area of significant research interest. Despite its simple structure, the leakage of contact static seals can have a direct impact on the operational safety of the device and can lead to environmental pollution and the waste of resources. Research has shown that even highly polished machine-processed sealing end faces are rough, which leads to inevitable leakage (Qiang et al., 2018).

The main problem is the influence of surface roughness on the contact mechanics at the seal-substrate interface. Most surfaces of engineering interest have surface roughness on a wide range of length scales (Persson, 2005), (from cm to nm) which will influence the leak rate and friction of seals, and accounting for the whole range of the surface roughness is impossible using standard numerical methods, such as the Finite Element Method. (Lorenz et al., 2009)

Looking at figure 3.2, we have P_a on the left which will be the pressure outside the submarine at a depth of 30 to 50 meters. On the right, we have P_b which is the pressure inside the submarine. The pressure difference is $\Delta P = P_a - P_b$ results in liquid flow or leakage at the interface between the rubber seal and the rough substrate surface. The leakage depends on the squeezing pressure P_0, the width, and the elastic modulus of the seal.

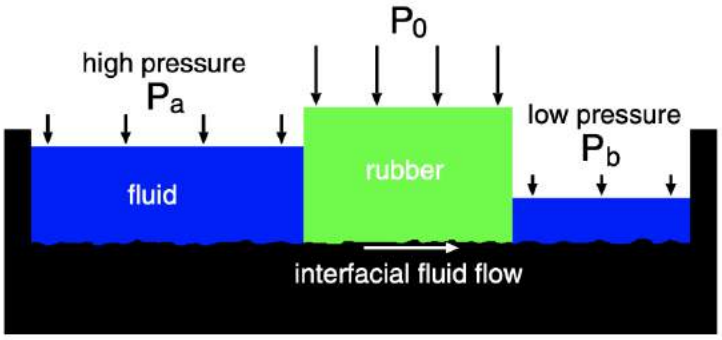

Figure 3.2: Schematic of the rubber seal that should prevent the fluid to flow to the lower pressure side. (Lorenz, 2009)

Roughness

Surface roughness, also known as roughness, is a property that pertains to the deviation of a surface profile in relation to a flat plane. Small deviations are classified as smooth with a small roughness, while large deviations are considered rough surfaces. In other words, any deviation from a perfectly flat surface is classified as roughness. This property plays a significant role in contact mechanics and, as such, has a critical impact on sealing. The effect of roughness is that

the true contact area between two surfaces is different from the nominal contact area. (Robert F. , 2015)

There are various ways to describe the roughness of a surface, with the unit most commonly used being the arithmetic average roughness (Ra). Mathematically, Ra is the arithmetic average value of the profile departure from the mean line within a sampling length. The Ra value is typically calculated from a set of data points that were collected from the surface of the material using a 3D optical profilometer, a device that can measure the surface profile of a material. The profilometer scans the surface of the material and records the height of each point along the scan path, which is used to calculate the average deviation of the surface from a perfect plane. It is a non-destructive technique that analyzes the surface topography of a specimen and generates a 3D profile. (Canning, 2020) The machine shines a light on the material and with its reflection, it can generate the digital surface roughness of the material.

It is important to note that the Ra value is only one of the several parameters that can be used to describe surface roughness. Other parameters, such as Rq, Rt, and Rz, also exist and are used in different fields, depending on the surface type and the application. For example, Rz is used to measure surfaces with high peaks and valleys that are more likely to be found in castings and forgings. It is also important to note that the Ra value does not take into account all features of a surface, such as waviness or form. Therefore, depending on the specific application or industry, different parameters may be more appropriate to use to describe the surface roughness. (NES, 2020)

In summary, the roughness profile parameters are Ra, Rz, Rp, Rv and Rq. Ra stands for the arithmetic mean deviation, Rz stands for the maximum peak height, Rp stands for the maximum profile peak height (above the mean profile line), Rv stands for maximum profile valley depth (below the mean profile line) and Rq stands for the root mean square deviation. It is important to note that in reality, a surface is not flat and contact is made up of a large number of asperities, where some are in contact, while smaller asperities on the surface are not in contact at all. (J.N.B. Huisman, 2017)

Zooming in on a ‘square’ of the contact surface results in less contact between the surfaces. This is called the magnification ζ. Which is defined as $\zeta = L/\lambda$ where λ is the shortest wavelength roughness that can be observed at the magnification ζ. And L is the length of the square (reference length). It can be seen in figure 3.3 that the contact region decreases when the magnification increases. (Lorenz, 2009)

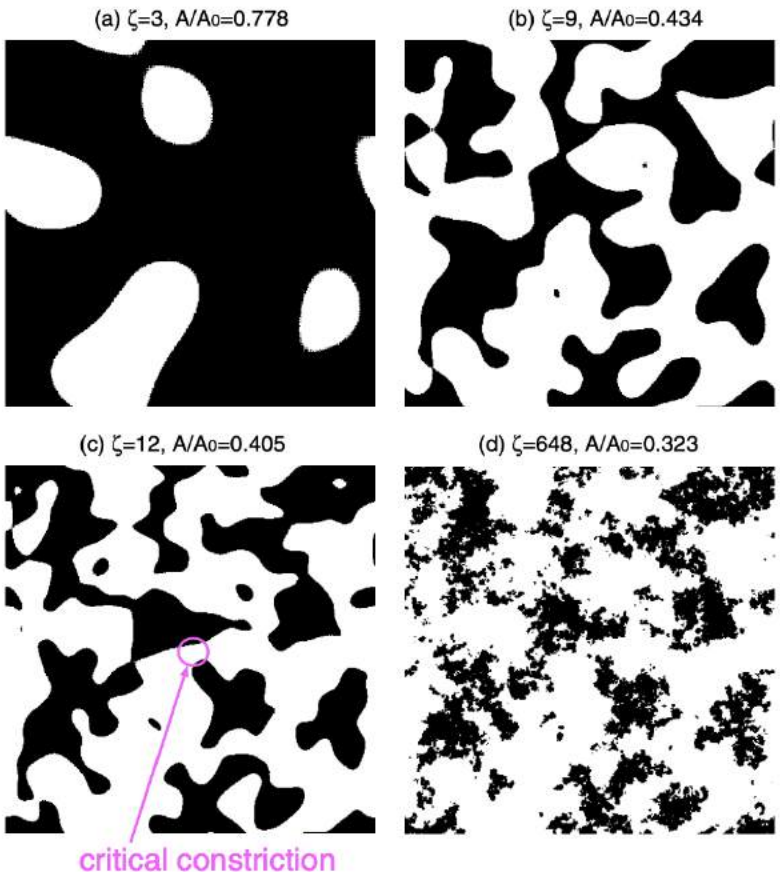

Figure 3.3: The contact region at different magnifications (ζ). (Lorenz, 2009)

Figure 3.4 shows a reference plane of a flange connection. Zooming in on the contact surface shows an increasing surface roughness. The figure shows the negative relation between the pore height and the contact load, and the positive relation between the pore height and leakage rate.

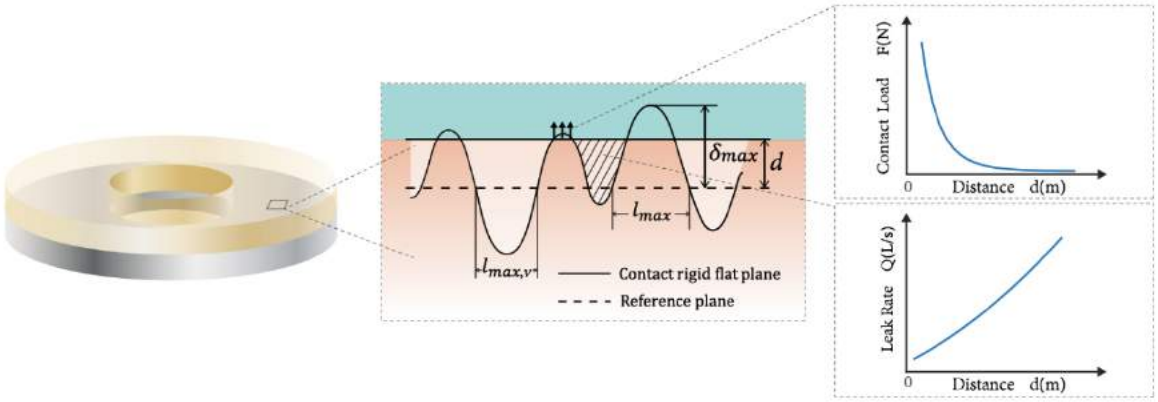

Figure 3.4: Schematic of the ring gasket leakage prediction model. (Qiang et al., 2018)

Recommended surface roughness for sealing

The recommended maximum surface roughness for sealing surfaces is 0.8 μm Ra, as per the research of Robert F. (2015). This value has been established as the optimal roughness for ensuring proper seal performance. However, it is important to note that in cases where the surface is subject to biofouling, the roughness of the growing biofouling is significantly larger than the recommended 0.8 μm, making it unrealistic to seal the surface effectively. As such, it is crucial to consider the presence of biofouling when evaluating the suitability of a surface for sealing applications.

4 Problem analysis

In this section, the problem context will be summarized. Moreover, the stakeholder will be analyzed and afterward, the problem statement will be discussed.

4.1 Problem context summary

Biofouling will inevitably grow on the top of the shaft causing a certain roughness that negatively affects sealing. Other factors affecting sealing are the width and the elasticity of the seal. It is found that the recommended surface roughness for sealing is 0.8 µm Ra. Besides, the average barnacle will grow in centimeters causing a roughness that exceeds the recommended sealing surface roughness for sealing.

Therefore, biofouling should be removed or prevented. It is found by desk research that the most common method used to remove biofouling from ship hulls is hydro blasting. However, it is unclear what surface roughness will remain after cleaning the surface.

4.2 Stakeholder analysis

This section will analyze the stakeholders. Four stakeholders are determined. This research is delegated by the Ocean Grazer BV and therefore, they are the problem owner. Three of the stakeholders are part of the Ocean Grazer team.

Drs. W.A. Prins is the founder and the scientific advisor of the Ocean Grazer BV. Besides, he is the daily supervisor of this research. He is the brain behind the OB and wants to commercialize this. Therefore, he has power and interest in this project.

Prof. dr. A. Vakis is the co-founder and the scientific advisor of the Ocean Grazer BV Besides, he is the first supervisor of this research. He is interested in the technical aspects of the research.

Marijn de Rooij is the CTO of the Ocean Grazer BV. He has a high interest in the results of the project, as this could increase the value of their product. They are also interested in the costs of the docking mechanism, as the system must be financially interesting. Marijn will provide material from the company which is useful to this project. He has less power in the project, as he does not interact directly with the research. Marijn has developed the OB and has an understanding of how the docking mechanism will look.

Finally, future investors/customers are of great importance. Because these investors are interested in the OB, they will also be interested in how maintenance will be done and what the costs will be. The investors will be interested as they will finance it, but they have less power.

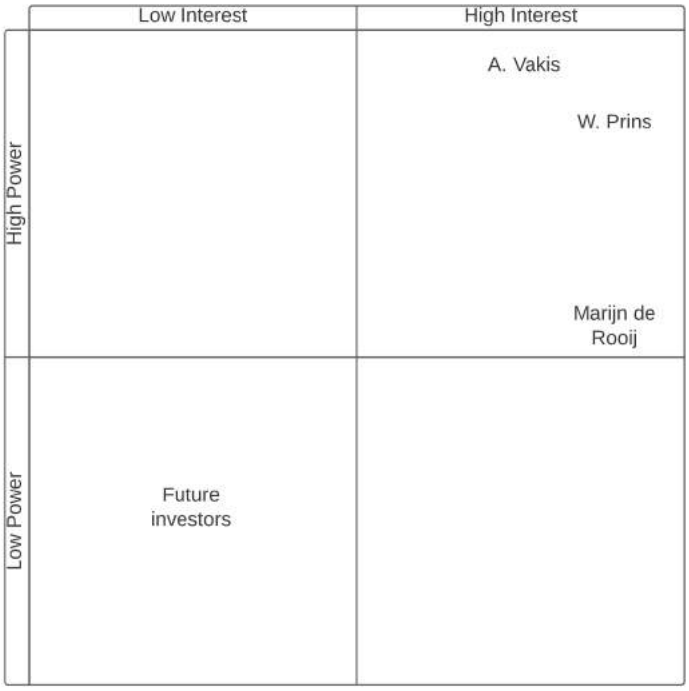

Figure 4.1: stakeholder analysis

4.3 Conceptual Model

Figure 4.1 shows the why-what model of the research. The problem is defined in red: it is unclear what the effect of biofouling is on sealing the docking mechanism. The question ‘what is stopping us from solving this problem?’ is asked in the right direction. And the question ‘Why do we want to solve this problem?’ is asked in the left direction. It becomes clear in the right direction that 1) the principles of sealing and 2) the effect of removing biofouling on surface roughness and the relation between these two need to be investigated by theory and an experiment.
Additionally, it becomes clear in the left direction that we want to solve this because maintenance engineers need to enter the OB shaft safely.

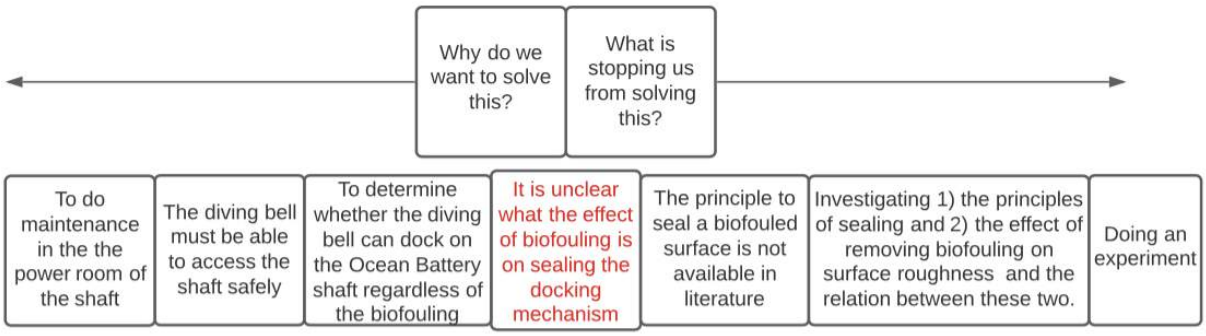

Figure 4.2: Why-what model

4.4 Problem statement

In order to access the OB shaft safely, the docking mechanism of the submarine should seal properly. After years, biofouling will grow on the shaft, causing high surface roughness. This roughness includes corrosion, barnacles, and sponges. It is unclear what surface roughness will remain after removing biofouling, what pressure (P0), and what seal is needed to be able to seal the OB shaft.

5 Research design

5.1 Research objective

The objective of this project is to investigate surface roughness after removing biofouling and its effect on sealing at a depth of 30-50 meters by setting up an experiment to replicate the docking mechanism on scale. To advise the Ocean Grazer BV on what the desired squeezing pressure is, whether this pressure is realistic to be obtained and on what seal this pressure will act to control an acceptable rate of leakage within 12 weeks.

5.2 Research questions

The previous section provided the problem and research objective. This section will list a set of research questions. The combination of the answers to these questions will reach the research objective.

Main Question

What is the surface roughness after removing biofouling and its effect on sealing the OB shaft?

Theoretical sub questions

- What is an acceptable leakage rate for submarine structures?
- How are the dimensions of the seal scalable? What is the relationship between the leakage rate and the width of the seal?

Empirical sub questions

- What is the range of surface roughness after removing biofouling?
- What is the relationship between hydrostatic pressure and leakage rate?
- What is the relation between the squeezing pressure and the leakage rate?
- What is the effect of surface roughness on sealing?
- What is the relationship between the seal's outer diameter and leakage rate?
- What is the desired squeezing pressure to reach an acceptable leakage rate? How could this pressure be obtained? And is this realistic?

5.3 Methods and Tools

In the previous section, research questions are set up. This section will elaborate on how the questions will be answered.
The main questions will both be answered by theoretical research and experiments.
The experiment will be set up by the experimental cycle which can be seen in figure 5.1.

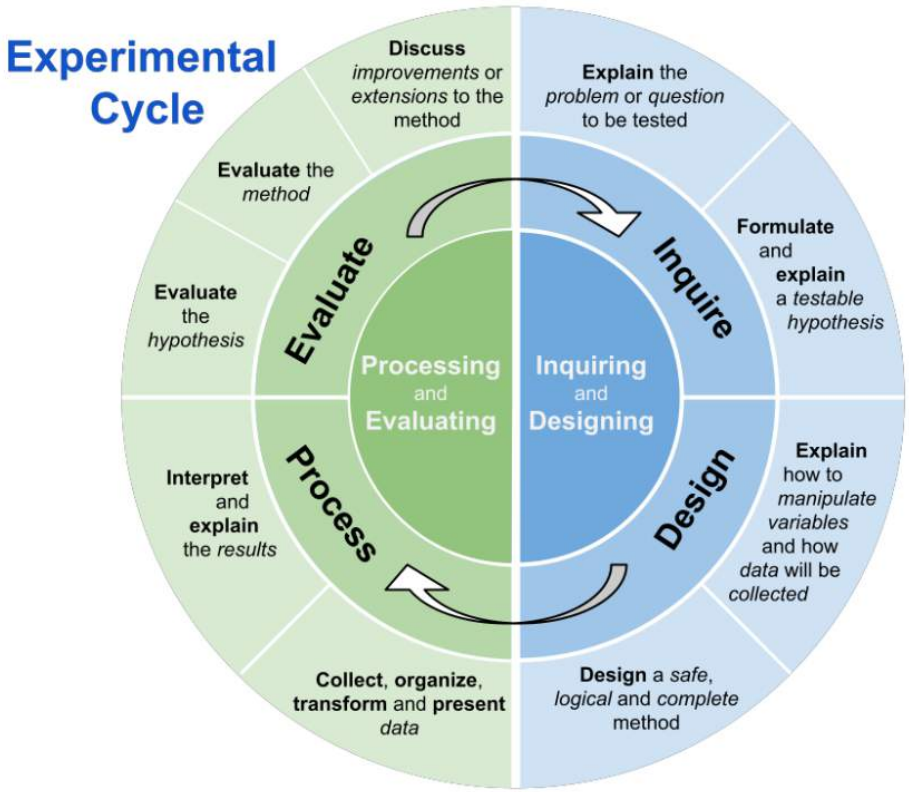

Figure 5.1: Experimental cycle including the steps taken for this report.

6 The experiment

This section adheres to the experimental cycle outlined in section 5.3, beginning with the identification of the problem to be examined and the formulation of a testable hypothesis. Subsequently, the design of the experiment will be discussed, including the manipulation of variables, data collection techniques, and specific procedures employed. The results will then be collected and analyzed, and the hypothesis will be evaluated based on the outcomes of the experiment. The process of the experimental cycle will be systematically followed to ensure rigorous scientific methodology and to ensure that the results are reliable and valid.

6.1 Questions being tested

The problem is explained in section 4. The research questions are provided in section 5. The question which will be answered in the experiment are the following:

- ➢ What is the relationship between the hydrostatic pressure and the leakage rate?
- ➢ What is the effect of surface roughness on sealing?
- ➢ What is the relationship between squeezing pressure and leakage rate?
- ➢ What is the relationship between the seal's outer diameter and leakage rate?

The first question is important to exclude whether the experiments should be done on one or more depths (or hydrostatic pressures). If there is a clear relationship, the leakage rates for one hydrostatic pressure can calculate the leakage rate for other depths. The second question is important because after removing biofouling, there will remain a range of surface roughness.The range of roughness that remains could be matched to the surface roughness used in the experiment. The third question is interesting for calculating the range of pressure needed on the seal for achieving the desired leakage rate. The fourth question is important to be able to scale the experiment to the real size of the OB.

These questions will be answered by two sets of experiments. Each measurement will be replicated three times. Replication is important for experiments because it helps to ensure that the results are accurate. When an experiment is replicated, it can help to verify that the initial results were not due to chance or some other variable. This allows researchers to make more accurate conclusions about the results of the experiment. Additionally, replication can also help to identify any potential flaws in the original experiment that may have resulted in inaccurate results.

6.2 Hypothesis

Question 1: What is the relationship between the hydrostatic pressure and the leakage rate? From the paper of Lorenz it becomes clear that the formula for the leakage flow is as follows:

$$\frac{d}{dt}Q = \frac{Ly}{Lx}\alpha\frac{u^3(\zeta c)}{12\eta}\Delta P \quad (4)$$

It can be concluded that the relation between the leakage rate and the ΔP is linear as the other factors in (4) are independent of the fluid pressure. This prediction is experimentally tested for pressure difference up to 10 KPa shown in figure 6.1.

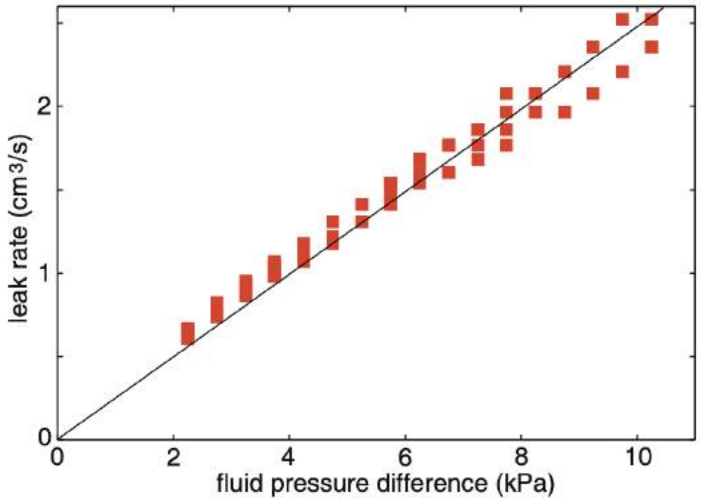

Figure 6.1: Linear relationship between the leakage rate and the fluid pressure difference under a nominal squeezing pressure of 60 KPa. For the roughness of a P120 sandpaper. Using a rubber seal with Young's elastic modulus of E = 2,3MPa. (Lorenz, 2010)

The relationship holds strictly true only if the microscopic strain in the asperity contact regions is similar to the macroscopic strain in the Hertz contact region (Persson, 2022). However, it is uncertain whether this holds if the fluid pressure difference changes with a factor of 10^3.

Question 2: What is the effect of surface roughness on sealing?

Rougher surfaces will cause higher leakage rates. The relative contact area between the seal and the rough substrate increases causing the overall pressure to decrease. Conversely, smoother surfaces can create a more uniform contact area resulting in a lower leakage rate.

Question 3: What is the relationship between squeezing pressure and leakage rate?

In general, it is expected that the relationship between the squeezing pressure and the leakage rate is negative; for increasing squeezing pressure, a decrease in leakage is expected. (Qiang et al., 2018)

This will happen until a certain point where no leakage occurs. At this point, increasing squeezing pressure will not affect the leakage rate.

Question 4: What is the relationship between the seal's outer diameter and leakage rate?

It is expected that the relationship between the seal's outer diameter and the leakage rate is negative. An increase in diameter will cause a decrease in leakage because the flow channel through which the water needs to percolate increases.

6.3 How to manipulate variables and collect data

In this section, the methodology of the experiments will be thoroughly explained, including the manipulation of variables, data collection techniques, and the specific procedures employed.

Squeezing Pressure: The manipulation of squeezing pressure will be achieved through the use of four bolts and four nuts, which will be tightened with a torque wrench as outlined in Appendix E. This ensures a consistent, stable, and quantifiable contact force on the seal. The total weight of the experimental setup will also be considered as a component of the squeezing pressure.

Surface Roughness: The surface roughness will be varied by utilizing three different sandpapers with 'roughness' of P40, P80, and P150. This classification system indicates the number of abrasive particles per square inch, with lower P numbers being classified as 'rougher'. The sandpapers will be optically analyzed using a 3D optical profilometer at the UMCG, as detailed in Appendix F. This instrument employs light direction techniques, by shining a red laser on the material and collecting the reflection of it to determine the profile of the surface. This analysis will be performed at each point in 5 square mm. The results of this analysis can be found in Appendix D.

Leakage Rate: The leakage rate will be measured in two ways, depending on the height of the leakage rate. For high leakage rates, the time will be measured for the transparent tube (Figure 6.2) to be completely emptied. For lower leakage rates, the height drop of the water level in the transparent tube will be measured in two minutes. The total volume of the transparent tube is 711.62 cubic cm, and the length of the tube is 27.5 cm.

Hydrostatic Pressure: The hydrostatic pressure will be manipulated by adding air pressure on top of the water. This air pressure will be generated by an air compressor and regulated by a pressure regulator. The height of the experimental setup will also be taken into account as an additional component of the hydrostatic pressure.

Seals: Three different seals will be utilized in the experiments, which can be found in Appendix B. The dimensions and material properties of these seals will differ.

6.3.1 First experiment

In the first experiment, the sample material utilized will be 150P sandpaper. The primary variable of interest is the squeezing pressure, which will be manipulated at two levels. Additionally, the experiment will be conducted on three distinct seals, with the hydrostatic pressure being systematically varied across four levels (1, 2, 3, and 4 bar). The leakage rate will be measured for each combination of squeezing pressure, seal, and hydrostatic pressure, thus allowing for the examination of the relationship between these variables.

6.3.2 Second experiment

In the second experiment, the variable of interest is the squeezing pressure, which will be systematically manipulated at four levels (10, 20, 30, and 40 KPa) while maintaining a constant hydrostatic pressure. Furthermore, the experiment will employ three different sorts of sandpaper (40P, 80P, and 150P) as the sample materials.

The results obtained from the first experiment are deemed to be of crucial importance in the design of the second experiment. If the initial experiment yielded evidence supporting a linear relationship between leakage rate and pressure difference, it would be appropriate to hold the pressure constant in the second experiment and utilize this linear relationship to predict the leakage rate at varying depths. However, if the first hypothesis was disproved, it would be necessary to conduct the second experiment at a pressure of 4 and 6 bar (corresponding to depths of 30 to 50 meters) in order to further investigate the relationship under examination.

6.4 Experimental setup

The design of the experiment was carefully considered in order to effectively investigate the effect of surface roughness on the sealing of an OB after removing biofouling. The schematic of the experimental set up is shown in figure 6.2. A flange connection was chosen as it closely mimics real-world situations, with the main differences being the direction of the pressure difference and the lack of bolt connections for the submarine. The experimental setup was constructed using PVC tubes and connecting parts that were able to withstand high pressures, and was designed with both controlled and measurement cells to accurately measure the leakage rate and time. The squeezing pressure was controlled by tightening bolt-nut connections with a torque wrench, and the surface roughness was controlled by adding analyzed sandpapers. The sealing cell was also carefully considered, with the seals being placed between the upper flange and the sandpaper, and the upper and blind flange being squeezed together by the bolt-nut connection. Overall, a thorough and well-designed experimental setup was implemented to effectively investigate the effect of surface roughness on the sealing of an OB after removing biofouling.

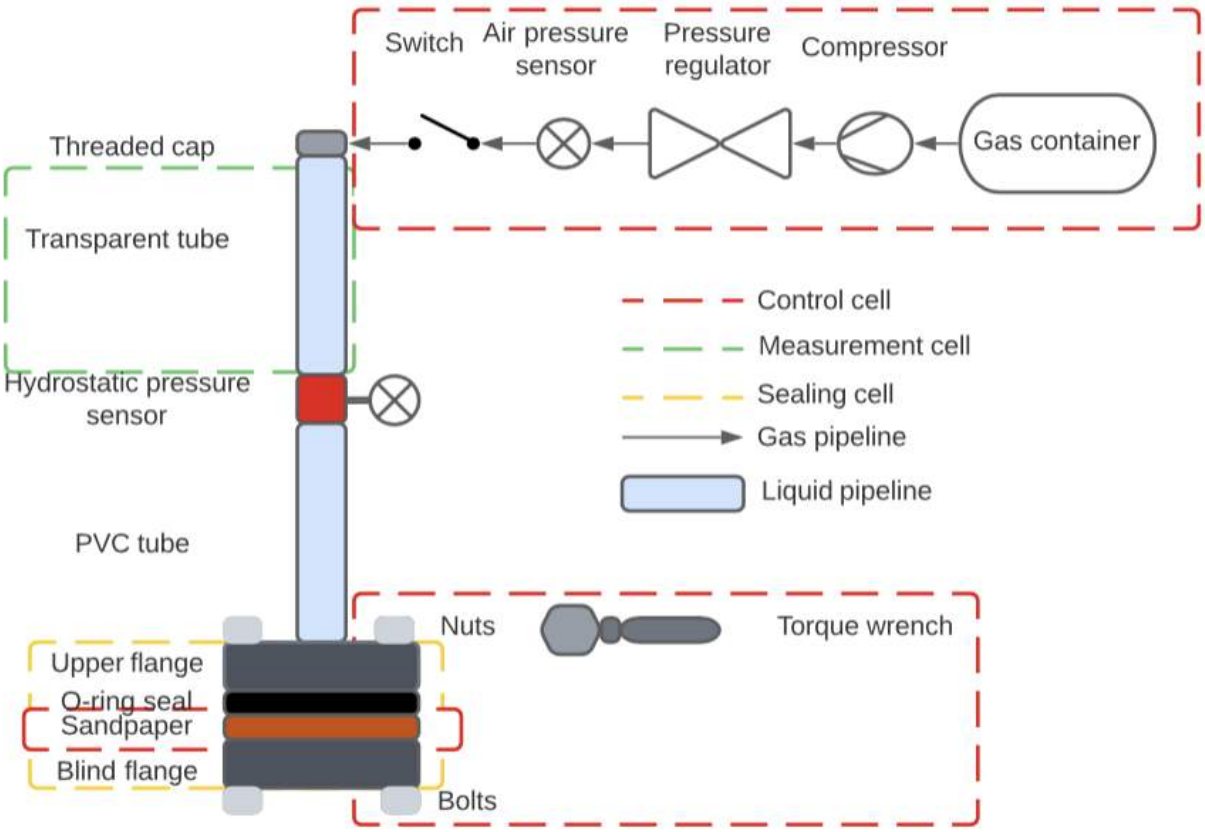

Figure 6.2: schematic of the experimental setup

6.5 Data acquisition and documentation

To ensure the validity and reliability of the experimental data, it is essential to establish a leveled experimental setup. In this study, the setup is aligned with a beam in the "Waterhall," the laboratory of the Ocean Grazer BV, utilizing a spirit level. To further ensure accuracy, each experiment is replicated three times, and the results are averaged. Error bars, representing the standard deviation of the three measurements, are included in the resulting graphs. Additionally, two sensors are employed to measure the hydrostatic and air pressures during the experiments. This methodology allows for a systematic and controlled approach to data collection, ensuring the validity and reliability of the results.

The relationship between the leakage rate and the water pressure is displayed in the graphs presented in Figures 6.3 to 6.6. The x-axis represents the water pressure, while the y-axis represents the leakage rate. The data points displayed in the graph are the result of multiple experiments, in which the water pressure was varied and the corresponding leakage rate was recorded.

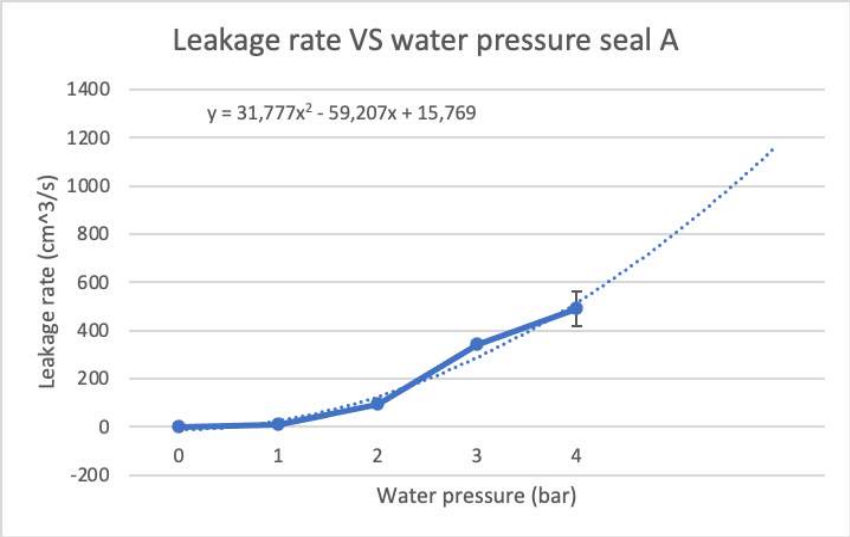

Figure 6.3: The relationship between the leakage rate and the water pressure for seal A for low squeezing pressure.

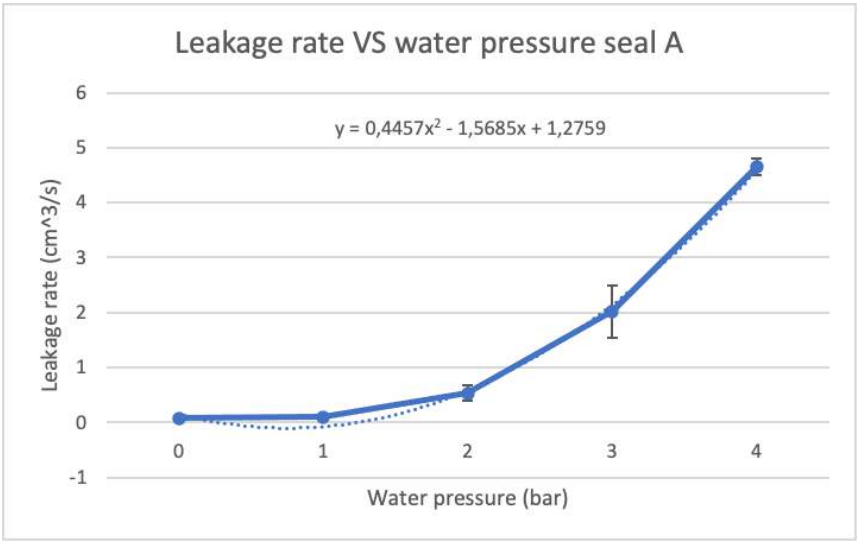

Figures 6.3 and 6.4: The relationship between the leakage rate and the water pressure for seal A for higher squeezing pressure.

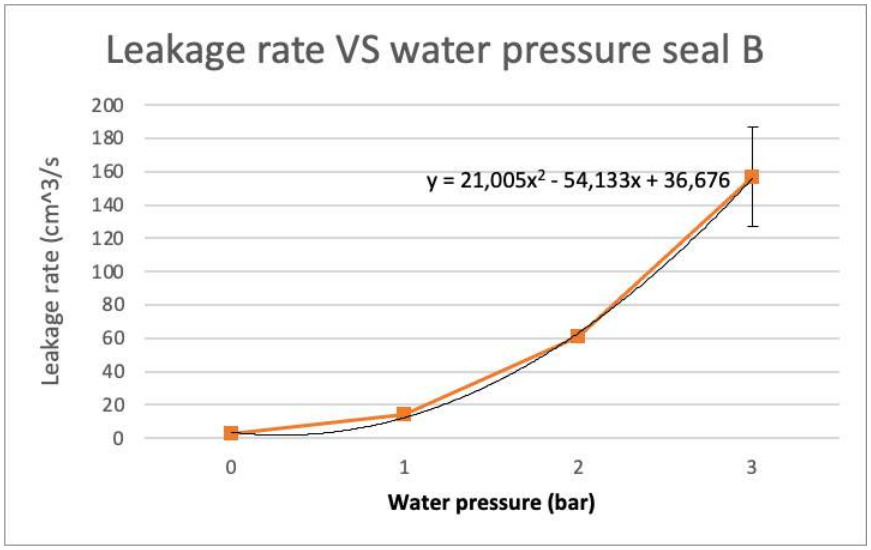

Figure 6.5: The relation between the leakage rate and the water pressure for seal B for low squeezing pressure.

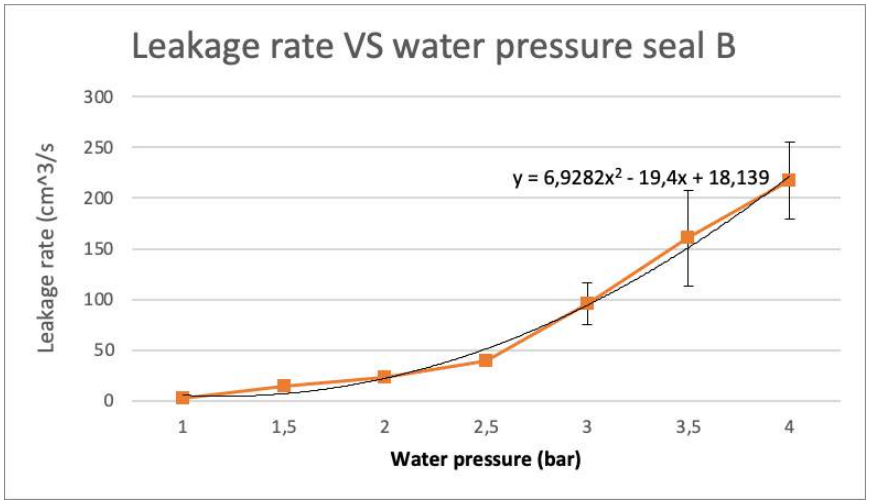

Figure 6.6: The graph shows the relationship between the leakage rate and the water pressure for seal B for a higher squeezing pressure compared to figure 6.5.

The following graphs show the results of experiment 2. The relationship between the leakage rate and the hydrostatic pressure, the squeezing pressure, surface roughness, and the seal's diameters is displayed in the graphs presented in Figures 6.7 to 6.12. The x-axis represents the squeezing pressure, while the y-axis represents the leakage rate. The data points displayed in the graph are the result of multiple experiments, in which the hydrostatic pressure, the squeezing pressure, the surface roughness and the seal's diameters were varied and the corresponding leakage rates were recorded.

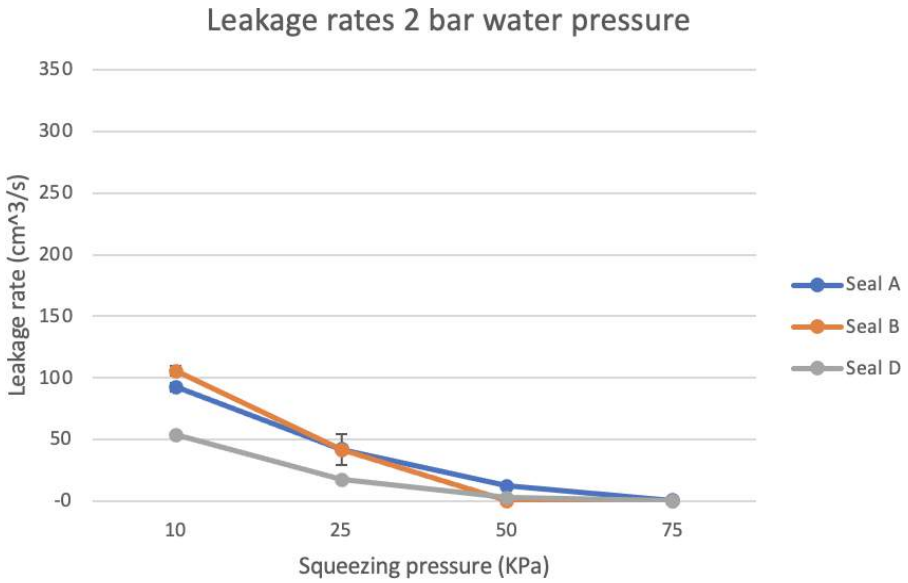

Figure 6.7: Leakage rates of seals A (blue), B (orange), and D (gray) with P40 sandpaper. The graph shows the results of the hydrostatic pressure of 2 bar.

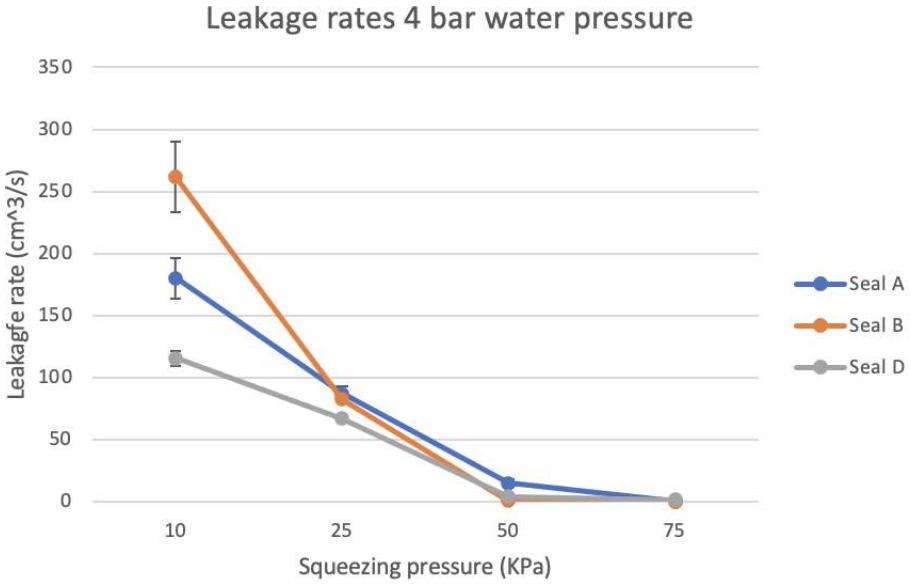

Figure 6.8: Leakage rates of seals A (blue), B (orange), and D (gray) with P40 sandpaper. The graph shows the results of the hydrostatic pressure of 4 bar.

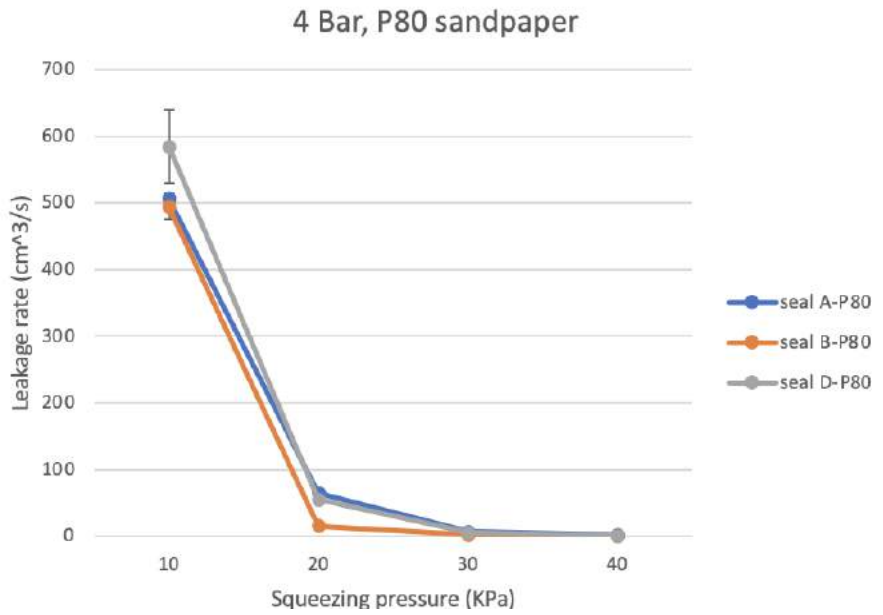

Figure 6.9: The leakage rate of seals A (blue), B (orange), and D (gray) with a hydrostatic pressure of 4 bar. The graph shows the results with the P80 sandpaper.

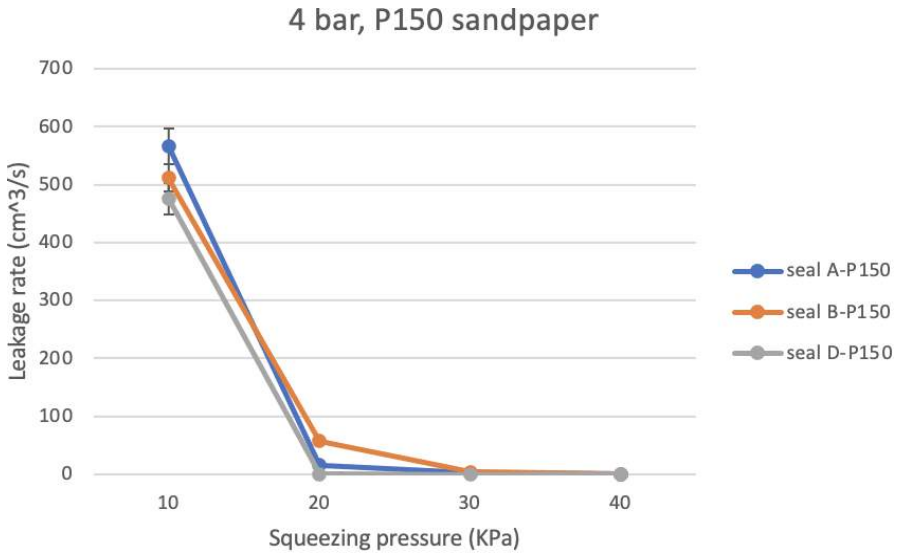

Figure 6.10: The leakage rate of seals A (blue), B (orange), and D (gray) with a hydrostatic pressure of 4 bar. The graph shows the results with P150 sandpaper.

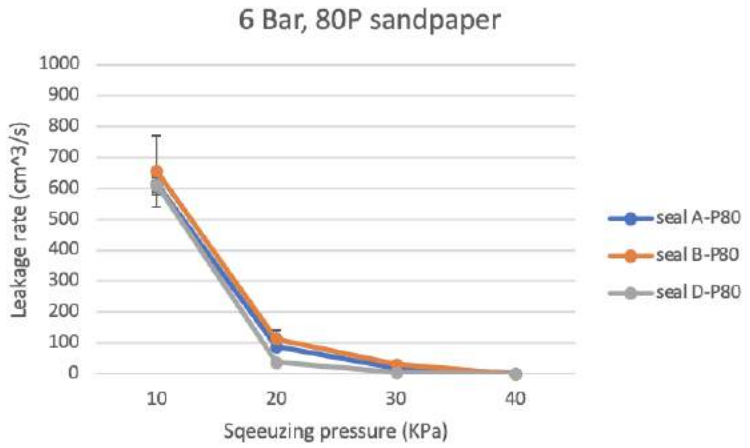

Figure 6.11: The leakage rate of seals A (blue), B (orange), and D (gray) with a hydrostatic pressure of 6 bar. The graph shows the results with 80P sandpaper.

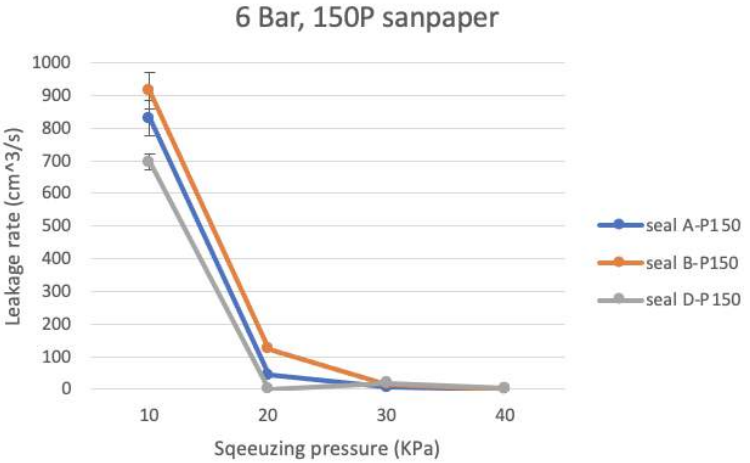

Figure 6.12: The leakage rate of seals A (blue), B (orange), and D (gray) with a hydrostatic pressure of 6 bar. The graph shows the results with 150P sandpaper.

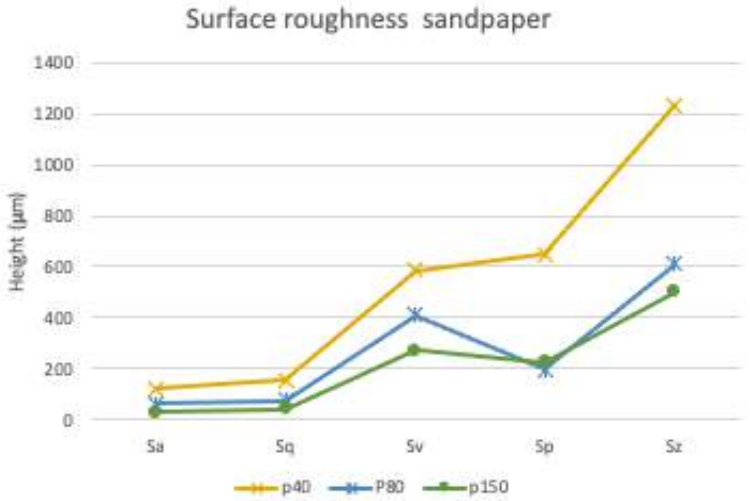

Figure 6.13: Surface roughness of sandpaper with the profile parameters: Sa stands for the arithmetic mean deviation, Sz stands for the maximum peak height, Sp stands for the maximum profile peak height (above the mean profile line), Sv stands for maximum profile valley depth (below the mean profile line) and Sq stands for the root mean square deviation.

6.6 Interpret and explain the results

It can be observed from the data presented in figures 6.3 through 6.6 that the relationship between the leakage rate and water pressure follows a positive second-order polynomial trend. An increase in water pressure results in an increase in leakage rate. Additionally, the rate of change in leakage is greater for lower squeezing pressures, indicating that higher water pressure leads to a larger increase in leakage rate for lower squeezing pressures.

In experiment 2, it can be deduced from the data presented in figures 6.7 through 6.12 that the relationship between leakage rate and surface roughness is negative. As surface roughness increases, leakage rate also increases. Furthermore, the outer diameter of the seal appears to play a crucial role in the leakage process. Figures 6.7, 6.8, 6.10, 6.11, and 6.12 show that seal B (orange line) displays the highest leakage rate due to smaller percolation channels and seal D (gray line) displays the lowest leakage rate due to larger percolation channels. The results also indicate that surface roughness is negatively correlated with squeezing pressure, with higher surface roughness resulting in higher relative contact area and lower squeezing pressure. Additionally, the change in leakage rate is observed to be faster for smaller outer diameter seals.

It should be noted that figure 6.9 shows the highest leakage rate for seal D which is not expected. These counterintuitive results may be due to various factors, such as experimental error or variations in the conditions of the experiments. Further analysis and interpretation of these results will be conducted in section 6.8 to determine the underlying causes of these observations and to draw accurate conclusions.

It can be inferred from Figure 6.13 that the P40 sandpaper has a higher level of surface roughness as indicated by the deviation of its Sv, Sp, and Sz values from those of the other sandpapers. The higher peaks and valleys, as well as the higher maximum peak height, indicate a more rough surface. This is further supported by the observation that higher squeezing pressures were required to achieve acceptable leakage rates with the P40 sandpaper, as seen in Figures 6.7 and 6.8. This suggests that the peaks on the P40 sandpaper were sharper than those on the other sandpapers, and thus required greater pressure to achieve an acceptable leakage rate.

6.7 Evaluate the hypothesis

This section will evaluate the hypothesis. The research questions for this experiment are listed below.

- ➢ What is the relationship between the hydrostatic pressure and the leakage rate?

- ➢ What is the effect of surface roughness on sealing?
- ➢ What is the relationship between squeezing pressure and leakage rate?
- ➢ What is the relationship between the seal's outer diameter and leakage rate?

The results of Experiment 1 indicate that the hypothesis that the deformation of the asperities is similar to the macroscopic strain in the Hertz contact region is not supported by the data. So, if the deformation of the asperity is significant, the simplified model of the asperities does not hold. (Lorenz, 2009) Furthermore, the relationship between leakage rate and water pressure was found to be non-linear. This suggests that the size of the percolation channel increases as a result of deformation of the rubber caused by higher water pressures. Moreover, the relationship between water pressure and leakage rate can be approximated by a second-order polynomial, indicating that for higher squeezing pressures, the rate of change in leakage decreases.

The results of Experiment 2 indicate that there is a negative relationship between leakage rate and surface roughness, as well as between squeezing pressure and leakage rate. Additionally, it was found that the change in leakage rate decreases at a faster rate for smaller outer diameters and that the leakage rate decreases over time due to increasing deformation in the rubber. However, it is difficult to establish an exact relationship between these variables due to the unpredictable nature of the leakage rates.

6.8 Evaluate the method

The experimental design employed in the present study was not completely waterproof, as evidenced by the leakage observed in Figure 6.13, where it was found that there was an approximate leakage rate of one drop of water every 5 seconds. This highlights the limitations of the experimental design in measuring small leakage rates, thus rendering the results of the tests for leakage rate as not entirely accurate.

Moreover, the connection between the experimental apparatus was replaced after a certain number of experiments, which led to an improvement in the accuracy of the results for the latter measurements. However, this also resulted in a loss of comparability between the different measurements, making it more challenging to draw accurate conclusions from the data. This limitation in the experimental design highlights the need for further research to improve the accuracy of the results and to establish more robust methods for measuring small leakage rates.

Figures 6.14 and 6.15: The plastic connection (6.13) to the pressure gauge in the water column was replaced by a metallic connection (6.14).

During the course of the experiments, it was observed that the seal and the sandpaper became contaminated. This contamination resulted in a reduction in the size of the percolation channels, which in turn led to a decrease in the leakage rate. Specifically, the water column was found to be filled with unwanted filth, which sank to the bottom and filled the percolation channels, thereby reducing leakage. This phenomenon can be observed in Figure 6.15. Additionally, the rubbers showed plastic deformation, with increasing time there is increasing deformation in the rubber and therefore a reduction of the percolation channels.

This contamination highlights the importance of implementing measures to prevent or minimize contamination in future experiments, such as using new sandpaper and seals for each measurement. This can be accomplished by using materials that are resistant to contamination, such as stainless steel, or by implementing cleaning protocols between measurements to ensure that the apparatus is free of filth. These measures would help to ensure that the results of future experiments are more accurate, reliable, and comparable.

Figure 6.16: Contamination of the sandpaper and seal after a set of experiments.

Additionally, it was observed that the inner diameters of the seals did not correspond with the inner diameter of the flange. Specifically, seal D was found to have an outer diameter that was 1.38 cm larger than the outer diameter of the upper flange. Although the total area of the flange is taken as the area that is squeezed, this discrepancy in diameter leads to a lower squeezing pressure on the outer 1.38 cm and enlarges the percolation channel. This means that the comparison between the diameters of the seals is still valid, however, calculations with the diameter of seal D will not be entirely accurate.

Furthermore, it was found that seals that were not precisely aligned with the upper flange caused a reduction in the percolation channels, leading to an increase in leakage rates. This phenomenon can be observed in Figure 6.16. As a result, the experiments were retaken when this occurred. It is important to note that this issue is more likely to occur with seal B, due to its smaller contact area. Mostly, the 6 bar hydrostatic pressure moved the seal away from the axis, causing the problem. Therefore, it is crucial to ensure precise alignment of the seals with the flange to ensure accurate and reliable results.

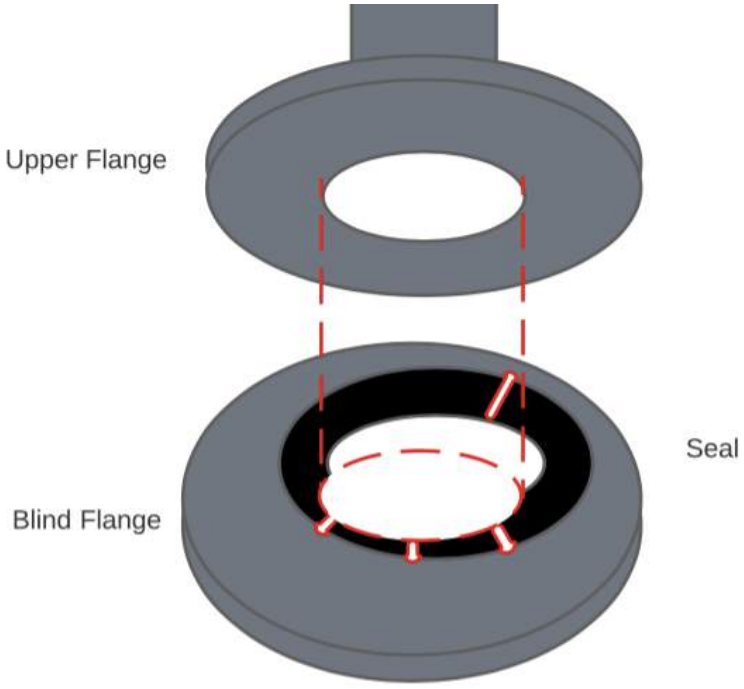

Figure 6.17: Schematic of a seal that is not precisely aligned with the upper flange, causing percolation channels to decrease, and therefore, the leakage rate to increase.

6.9 Improvement

Potential improvements to the experimental methodology include implementing measures to eliminate contamination from the sandpaper, such as using new sandpaper for each measurement. Additionally, it is crucial to ensure precise alignment of the seal with the flange, in order to accurately measure the leakage rate.

In addition, the influence of temperature on the leakage rate should also be considered. Research has established that temperature can have a significant effect on the leakage rate, and it is important to control the temperature of the water and seal in the experiments. (Chen Y et al., 2020) .However, in the current study, the temperature of the water in the water hall was not constant, due to issues with the heating system, which resulted in temperatures declining to around 0 degrees Celsius on some days and rising to around 15 degrees Celsius on others. In order to improve the accuracy of the results, it is essential to ensure that the temperature of the water and seal is kept constant during the experiments.

7 Acceptable leakage rate Tightness class

This chapter elaborates on an acceptable leakage rate for different industries and countries. Furthermore, this chapter will explain the acceptable leakage rate that is chosen as a standard for the submarine-OB connection.

In theory, there is no link without some level of fugitive emissions. Even solid materials are not "tight", and the "leakage" of metals can be described by their permeability. A connection is tight when it meets the sealing criteria defined by codes, system specifications, and vessel operator/customer requirements. Tightness is an important criterion for all types of connections in every pressure system and is part of the function of the connection. Actual "tightness" criteria may vary for different applications and design codes used. For example, even high leak rates are acceptable in stationary steam power applications.
The acceptable leakage rate for underwater structures is dependent on the type of structure and the purpose for which the structure is used. For example, the acceptable leakage rate for a dam may be significantly lower than the acceptable leakage rate for a pipeline. Generally, the leakage rate for a structure should be as low as possible to achieve the desired outcome. According to André M. et al., the acceptable leakage rate is zero for underwater safety valves for offshore service (API 6AVI 1994). This project will consider the sealing of the submarine to the OB shaft as a flange connection because this connection is also used in the experiment. And therefore, this report will take into account the leakage standards for flange connections.

There are currently no industry accepted methods for calculating the sealing effectiveness of flange connections during the research and development phase of a project. As there are many different designs of bolted piping connectors being widely used in the oil and gas industry, operators and regulators could benefit greatly from a more accurate comparison and estimate of expected flange tightness level, based on design calculations only. The tightness requirement depends on many factors: medium (toxic, explosive, radioactive, inflammable), design conditions (pressure temperature, joint size), sealing materials (metal to metal seals, Teflon/elastomer gaskets), consequences (pollution, loss of medium, system re-tightening or connection replacement request) and legal restrictions. (Przemyslaw Lutkiewicz et al., 2019)

The acceptable leakage rate of flange connections can be determined by the applicable industry standards, such as International standards (ISO), European sealing association (ESA)/ Fluid sealing association (FSA), American Petroleum Institute (API), American National Standards Institute (ANSI), Deutsches Institut für Normung (DIN), European Union (EN) or the Norwegian oil and gas recommended guidelines for good integrity (OLF 117).

The acceptable leakage rate can be defined as the tightness of a system. The unit is mg/(s m) which is the mass flow (mg/s) per meter of the mean perimeter of the gasket.
The American Society for Testing and Materials (ASTM) tightness classes are derived as:

- T1 Economy = Flange leakage rate of 2*10^-1 mg/(s mm)
- T2 Standards = Flange leakage rate of 2*10^-3 mg/(s mm)
- T3 Tight = Flange leakage rate of 2*10^-5 mg/(s mm)

(The European sealing association (ESA), 2009)

For this project, the T1 class will be chosen to be the acceptable leakage rate. Which is equal to 0,0457 cm^3/s. This standard is chosen because the experiments are also done with a flange connection. This tightness criterion is similar to the connection of the submarine to the OB.

8 Scalability

This section aims to explore the applicability of the experimental results to the real-world scenario of the submarine's connection to the OB. The flange connection used in the experiment has an inner and outer diameter of 4 mm and 7.28 mm respectively. To apply the results of the experiment to the real-world scenario, it is necessary to scale the dimensions of the flange connection to the size of the connection between the submarine and the OB.

It is important to note that the hydrostatic pressure and surface roughness are similar between the experiment and the real-world scenario. Additionally, it is assumed that the same type of seal will be used in the real-world scenario, with the only difference being the dimensions of the seal. As the dimensions of the seal are scaled up, the total contact area will increase, and the nominal force will also need to increase in order to maintain constant pressure.

It is assumed that the percolation channels will hold the same size and that the squeezing pressure will also be the same at the OB. According to the leakage standard of 2*10^-1 mg/(s mm), the acceptable leakage rate is linearly scalable with the perimeter of the flange. In other words, as the perimeter of the flange increases, the number of percolation channels increase, and the amount of leakage will increase. However, this increase in leakage is relative to the size of the flange and is still within the acceptable region.

In this analysis, two hypothetical scenarios will be considered in order to explore the applicability of the experimental results to a real-world scenario of the submarine's connection to an oil barrel (OB). The first scenario involves engineers entering the OB's shaft, while the second scenario involves replacing components in the OB.

For the first scenario, in which engineers will enter the OB's shaft, the inner diameter of the flange is scaled to 1 meter. It is assumed that the percolation channels will maintain the same length, and thus the difference between the inner and outer diameter of the upper flange is taken into consideration. The outer diameter is calculated to be 1.0328 meters, resulting in a total relative contact area of 0.05237 square meters. To generate a pressure of 40 KPa on the seal, a nominal force of 2094.8 N must be uniformly applied. Additionally, the increase in diameter results in an increase in the acceptable leakage rate to 0.648 cm^3/s.

In the second scenario, in which components are replaced in the OB, the inner diameter of the flange is scaled to 5 meters. Similar to the first scenario, it is assumed that the percolation channels will maintain the same length, and the difference between the inner and outer diameter of the upper flange is taken into account. The outer diameter is calculated to be 5.0328 meters, resulting in a total relative contact area of 0.2585 square meters. To generate a pressure of 40 KPa on the seal, a nominal force of 10340 N must be uniformly applied. Additionally, the increase in diameter results in an increase in the acceptable leakage rate to 3,16 cm^3/s.

9 Surface roughness of steel

This chapter will elaborate on how the piece of steel is collected and analyzed. Moreover, this chapter will elaborate how this piece of metal can be compared with the sandpapers used in the experiments.

The piece of steel is collected at the dockyard in Delfzijl. The company does maintenance on large ships. The outer surface of the ship is made of steel and after years, barnacles and sponges will grow there. When a ship is damaged, the company in Delfzijl cleans the outer surface with a high-pressure washer and replaces pieces of steel. A small part of such a ship hull is collected and shown in appendix J.

The Surface roughness of the steel sample is analyzed by the 3D optical profilometer at the UMCG and the results are shown in appendix G. Two parts of the sample are analyzed. The first part seemed ‘smooth’ and its roughness was measured to be 13,86 Ra.
The other analyzed part was showing some grains of sand that seemed ‘rough’ and its roughness was measured to be 167,34 Ra.

From this, it can be assumed that the surface roughness of ‘cleaned steel’ ranges from 10 to 200 Ra. Comparing this to the sandpapers used in the experiments, it can be concluded that the experiments did not include the whole range of surface roughness. Because the roughest sandpaper available (P40) has a surface roughness of 122,92 Ra, and some smoother sandpaper (P150) with a surface roughness of 31,85 Ra.

10 Squeezing pressure

This section will provide an analysis of the desired squeezing pressure for the flange connection between the submarine and the OB shaft, based on the desired leakage rate. Additionally, it will compare the surface roughness of the cleaned steel sample to the surface roughness of the sandpapers used in the experiments, as well as outlining methods for achieving the desired squeezing pressure.

According to S. Lassesen (2002), a criterion for the squeezing pressure of a flange is that it should be two times higher than the inner pressure. In the case of the submarine, the outer pressure is a maximum of 6 bar, thus the squeezing pressure should be at least 1.2 MPa.

However, as outlined in Chapter 7, the T1 Economy standard for flanges will be used. This standard states that the acceptable leakage rate for flanges is 2*10^-1 mg/(s mm), which is equivalent to a leakage rate of 0.0457 cm^3/s. Comparing this to the results of the experiments in Figure 9.1, it can be seen that seals B and D have an acceptable leakage rate at 4 bar hydrostatic pressure when using the P150 sandpaper.

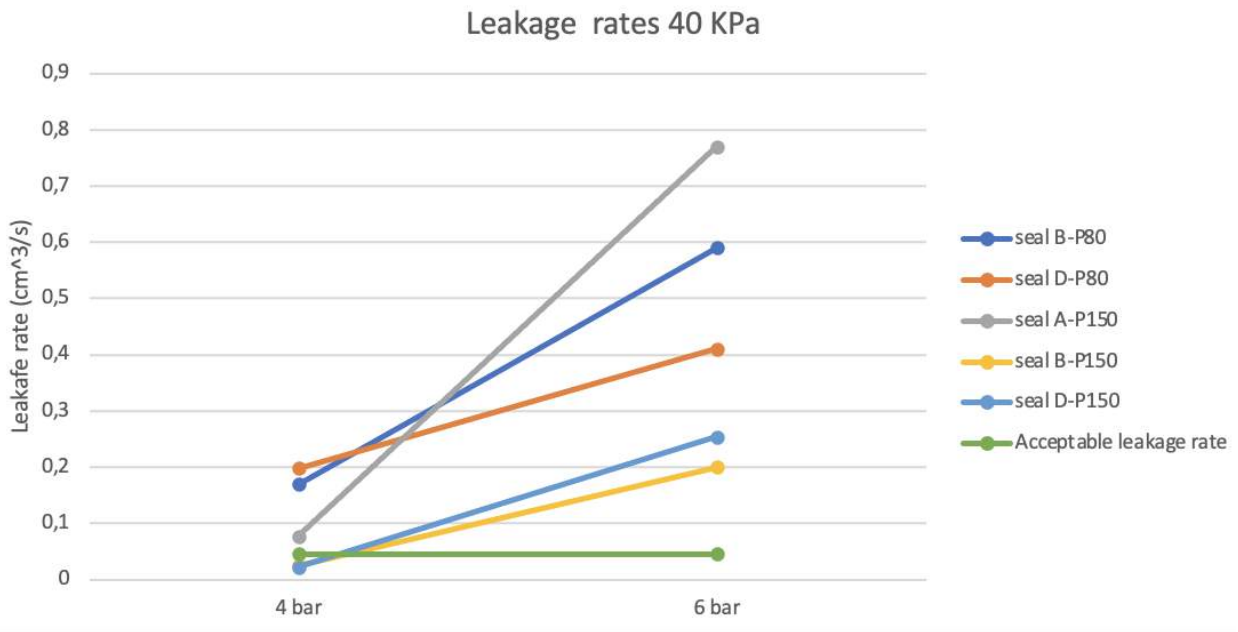

Figure 9.1: leakage rates with 40 KPa squeezing pressure for 4 bar hydrostatic pressure on the left, and 6 bar hydrostatic pressure on the right.

The data points were analyzed and it was concluded that the measurements at 4 bar hydrostatic pressure, with a squeezing pressure of 40 KPa, and surface roughness of 31.85 Ra on seals B and D were significant. However, other measurements were not within the acceptable leakage rate and thus were not considered significant.

Several methods are commonly used to generate pressure on underwater structures, including the use of hydraulic presses and inflatable seals. These two methods will be discussed.

Hydraulic presses are a sort of machine that uses a fluid to generate compressive pressure. Oil is the fluid normally used and is saved in a reservoir and is then pumped right into a cylinder, in which it exerts pressure on a piston. The piston then applies this pressure to a surface. The use of a hydraulic press is beneficial for applications that require high force over a small area, as the fluid in a hydraulic press can be easily and precisely controlled to generate high pressures. The accepted international standard for maximum working pressure in the high-pressure hydraulic tools industry is 700 MPa. (All Phase Hydraulics) This exceeds the desired squeezing pressure of the seal and is thus applicable for both scenarios.

Inflatable seals, on the other hand, are a type of seal that uses pressurized air or gas to create a sealed surface. They are typically made of rubber or other flexible materials and can be easily deployed, accurately generate pressure at the surface, and require relatively low maintenance. However, a rough surface with sharp edges could cut the rubber causing deflation. According to Advanced Sealing Technology, the seal could expand by 9 mm and could generate a maximum pressure of 300 KPa. This exceeds the desired squeezing pressure of the seal and is thus applicable for both scenarios.

It should be noted that for the use of inflatable seals, the submarine must be positioned above, and precisely aligned with, the OB by a clamping mechanism before the seal is inflated.

11 Conclusion

This chapter will summarize the project. It will discuss the inaccuracies and limitations of the experiment, recommendations for future research, and finally, this chapter will give the conclusion.

11.1 Discussion

The data considering the surface roughness after removing biofouling and the acceptable leakage rate were collected after the experiments were carried out. Therefore, assumptions were made before the experiments.

It was assumed that the surface roughness after removing biofouling would range between the roughest sandpaper available (P40) with a surface roughness of 122,92 Ra and some smoother sandpaper (P150) with a surface roughness of 31,85 Ra. However, after collecting and analyzing the cleaned surface, it became clear that the surface roughness ranges between 10 and 200 Ra. Meaning that the tested sandpapers do not include the entire range of surface roughness.

Besides, it was assumed that 0,5 cm^3/s would be an acceptable leakage rate as this would take almost two minutes for the water level to drop 2 cm in the transparent tube. However, after the experiments, it was found that the acceptable leakage rate for this flange is 0,0457 cm^3/s. This leakage rate is only measured two times.

Another point of discussion is the seals used. The company Advanced Sealing Technology recommended the use of an inflatable seal for this project. However, the costs of such a seal with a diameter of the flange used in the experiment are 600 Euro. This is expensive and therefore flange seals are used for the experiments.

Furthermore, the material characteristics of the rubber seals are known. The seals are given to the laboratory to be analyzed by a tensile tester. However, there is a high demand for the use of this machine resulting in unexpectedly long waiting times. Although the stress-strain curve of the materials is unknown, the plastic deformation under the same conditions can be compared. The maximum pressure on all materials is 40 KPa and the surface roughness to which it is pressed is also the same. Figure 11.1 shows the plastic deformation of the seals corresponding to the amplitude parameters of surface roughness. It can be concluded that the materials show similar plastic deformation and therefore have similar yield strength, ductility and a similar deformation mechanism. The plastic deformation is analyzed with the same 3D optical profilometer and the results are shown in appendix H.

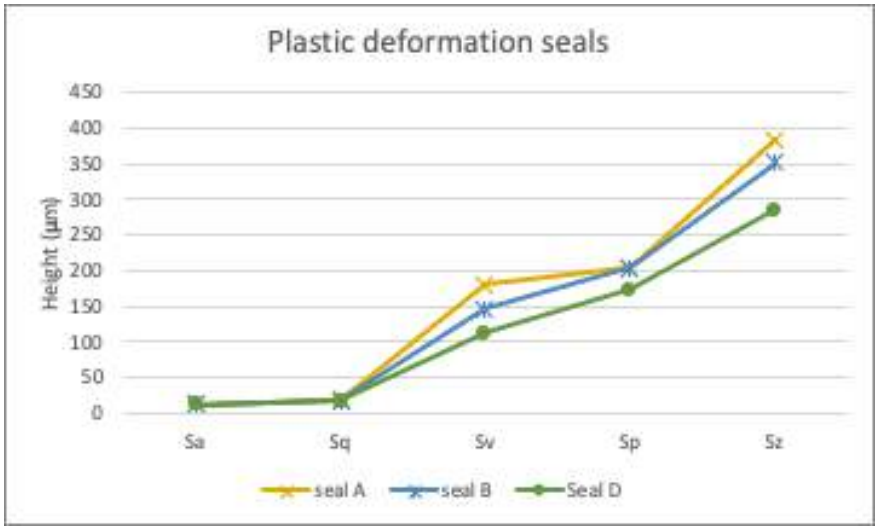

Figure 11.1: Comparison of plastic deformation of seal A (yellow) seal B (blue) and seal D (green). Corresponding to the amplitude parameters of the surface roughness.

11.2 Limitations

The first experiments were taken in absence of an applicable torque wrench. The torque wrench with the right scale was ordered later. Therefore, the squeezing pressure of the first results is unknown.

Furthermore, the first experiments were taken without a watertight setup. The leaking part is replaced after some time, resulting in an inaccuracy of comparing the results.
Also, the seal was not precisely aligned with the upper flange in some experiments.

Moreover, the temperature in the waterhall was near zero degrees celsius sometimes. The other experiments were taken at a temperature of 20 degrees Celsius. This influences the sealing and results in inaccuracies in comparing the results.

The leakage rate is measured intuitively till a certain point of ‘acceptance’. However, when the actual acceptable leakage rate according to the ATMS was found, only two data points correspond to that.

The piece of steel was collected at the end of the project, showing a surface range of roughness of 13,86 Ra to 167,34 Ra. The samples of sandpaper that were used in the experiments were ranging from 31,85 Ra to 122,92 Ra.

11.3 Conclusion

In conclusion, Energy Storage Systems (ESS) are of significant importance for the renewable energy industry. The Ocean Grazer BV has developed an innovative ESS solution called the Ocean Battery (OB), but challenges arise when it comes to safely entering the OB for

maintenance as it is located at the bottom of the ocean. Submarine rescue vehicles have been proposed as a potential solution, but the main challenge is the unwanted growth of biofouling on the OB which affects the ability to make a watertight connection by the submarine.

The growth of biofouling organisms such as barnacles and sponges on the OB can cause problems with sealing the connection between the submarine and the OB. An experiment was designed to replicate this connection and investigate the effect of surface roughness after removing biofouling on the sealing. Various variables were manipulated and analyzed, including squeezing pressure, surface roughness, leakage rate, seal dimensions, and hydrostatic pressure.

It was found that the relation between hydrostatic pressure and leakage rate is not linear, and that larger seals have overall lower leakage rates as the percolation channels increase. Additionally, it was found that the smaller the seal, the larger the change in leakage rate and that higher squeezing pressures reduce the leakage rate. Furthermore, the acceptable leakage rate for the submarine-OB connection is chosen as the T1 class, with a flange leakage rate of 0.0457 cm^3/s. However, only two measurements were within the acceptable leakage rates. Moreover, the range of surface roughness (Ra) of the collected steel after removing the biofouling is found to be 10 to 200 μm.

The experiment was scaled to match the size of the actual submarine-OB connection, and it was concluded that the desired contact pressure can be easily reached by hydraulic presses or inflatable seals. Overall, this project has provided valuable insights into the effect of surface roughness on the sealing of a flange connection after removing biofouling.

11.4 Recommendations

In this project, several experimental set-up problems were encountered resulting in less accurate outcomes. It mainly concerned the desired leakage rate and the measured surface roughness of the collected steel.

The results of this project have provided valuable insights into the effect of surface roughness on the sealing of a flange connection after removing biofouling. However, it has also highlighted the need for further studies with improved experimental set-up to increase the significance of the results. Therefore, it is recommended that future research should focus on gathering all necessary information before starting the experiment, arranging for the use of necessary machines at the beginning of the project, and ensuring proper alignment of the seal during the experiment and in the actual connection of the submarine and the OB shaft. Experiments should be conducted within the acceptable leakage rate and relative to the surface roughness of the cleaned OB shaft. More research can also be done on underwater surface cleaning, ensuring a certain range of surface roughness. And the docking mechanism should be designed further, considering a clamping mechanism that generates uniformly divided pressure over the seal.

Additionally, more research should be conducted on the squeezing pressure needed for rougher substrates, the use of inflatable seals, and the strength of the docking mechanism and the OB shaft to ensure structural safety and prevent leakage. Overall, the goal should be to achieve the acceptable leakage rate that is comparable to that of the connecting flange.

References

AB Gallo, JR Simões-Moreira, HKM Costa, MM Santos, and E Moutinho dos Santos (2016). Energy storage in the energy transition context: A technology review. Renewable and sustainable energy reviews, 65: 800–822, 2016.

Abioye, O.P., Loto, C.A. & Fayomi, O.S.I. (2019). Evaluation of Anti-biofouling Progresses in Marine Application. *J Bio Tribo Corros* 5, 22 . https://doi.org/10.1007/s40735-018-0213-5

Albitar, Houssam & Dandan, Kinan & Ananiev, Anani & Kalaykov, Ivan. (2016). Underwater Robotics: Surface Cleaning Technics, Adhesion and Locomotion Systems. International Journal of Advanced Robotic Systems. 13. 1. 10.5772/62060.

All Phase Hydraulics. What is Hydraulic Pressure and Why is it Important? - All Phase https://www.allphasehydraulics.com/what-is-maximum-hydraulic-pressure-and-why-is-it...

Andrei G. Shvarts, Vlaidslav A. Yastrebov. (11 february, 2021). Contact mechanics and Elements of Tribology Lecture 8. Lubrication and Sealing
CES Innovation Awards Program Amsterdam Honorees - CES 2022
https://www.ces.tech/Innovation-Awards/Paris-Amsterdam-Innovations.aspx

André M. Barajas, David B. Walter, J, Christopher Buckingham. 1999. Allowable Leakage Rates And Reliability Of Safety And Pollution Prevention Equipment. MMS contract No. 1435-01-97-CT-30880

AZanimals. (2022), barnacles. https://a-z-animals.com/animals/barnacle/ [online accessed 28/10/22]

B N J Persson and C Yang J.(2008). Theory of the leak-rate of seals. Phys.: Condens. Matter **20** 315011

Callow, M.E.; Callow, J.E, 2002. Marine Biofouling: A Sticky Problem. *Biologist (London)*, *49*, 10–14.

Candries M, Atlar M, Weinell CE, Anderson CD. (2001). Low energy surfaces on high speed craft. In: Bertram V, editor. Proc 2nd Euroconference on High-performance Vehicles HIPER ’01. Hamburg: TUHH Technologie GmbH. pp 119 – 127.

Candries M, Atlar M, Mesbahi E, Pazouki K. (2003). The measure- ment of the drag characteristics of tin-free self-polishing co- polymers and fouling release coatings using a rotor apparatus. Biofouling 19(Suppl.):27 – 36.

Canning, C. (2020). Corrosion and biofouling of offshore wind monopile foundations(doctoral dissertation, university of edinburgh).

Chao Li , Gang Wang, Kaiyun Chen, Peng Jia, Liquan Wang, Xiangyu Wang and Feihong Yun. 2020**.** Analysis of Removing Barnacles Attached on Rough Substrate with Cleaning Robot. Journal of marine science and engineering.

ChemPro (2016). Degradation. https://www.chemsafetypro.com/Topics/CRA/ degradation.html. [Online; accessed 20-Oktober-2022].

Chen, Y., Li, D., Zhang, Y., Li, Z., & Zhou, H. (2020). The Influence of the Temperature Rise on the Sealing Performance of the Rotating Magnetic Fluid Seal. *IEEE Transactions on Magnetics, 56*, 1-10.

Dickon Howell & Brigitte Behrends (2006) A review of surface roughness in antifouling coatings illustrating the importance of cutoff length, Biofouling, 22:6, 401-410, DOI: 10.1080/08927010601035738

Environment – Assessment of Current and Emerging Approaches. Cawthron institute, New Zealand. Frontier ins marine science.

European Sealing Association (ESA) and Fluid Sealing Association (FSA). 2009. Flange Gaskets- Glossary of terms.

Grant Hopkins, Ian Davidson, Eugene Georgiades, Oliver Floerl, Donald Morrisey and Patrick Cahill. 2021. Managing Biofouling on Submerged Static Artificial Structures in the Marine

Gu, J.-D. (2005). Chapter 9 - biofouling and prevention: Corrosion, biodeterioration and biodegradation of materials. pages 179–206.

Hu, P., Xie, Q., Ma, C., and Zhang, G. (2020). Silicone-based fouling-release coatings for marine antifouling. *Langmuir* 36, 2170–2183. doi: 10.1021/acs. langmuir.9b03926

J. Franssen (2022), Determining the integrity of the flexible bladder under marine underwater conditions. Engineering and Technology institute. University of Groningen.

J.N.B. Huisman. (2017).The effect of crystal structure on nanoscale roughness. Engineering and Technology institute. University of Groningen

Kailey N. Richard *, Kelli Z. Hunsucker, Harrison Gardner, Kris Hickman and Geoffrey Swain. 2021. The Application of UVC Used in Synergy with Surface Material to Prevent Marine Biofouling. Center for Corrosion and Biofouling Control, Florida Institute of Technology, Melbourne, FL 32901, USA *J. Mar. Sci. Eng. 9*(6), 662; https://doi.org/10.3390/jmse9060662

Kyei, S., Darko, G., and Akaranta, O. (2020). Chemistry and application of emerging ecofriendly antifouling paints: a review. Journal of Coatings Technology and Research, 17:1–18.

Lorenz B. and Persson B.N.J. (2009) Leake rate of seals: Comparison of theory with experiment. EPL 86 44006

M. A. Hassink. (2016). Design of experimental measurements to obtain performance characteristics of a multiple ball check valve. Engineering and Technology institute. University of Groningen

Moresteam.(2016).Knowledgecenter-Toolbox.
https://www.moresteam.com/toolbox/design-of-experiments.cfm

National Ocean Service at National Oceanic and Atmospheric Administration U.S Department of Commerce, “What are Barnacles?,” 2017. [Online].

NES. 2020. What are the benefits of inflatable seals? -. (2020, September 21). Retrieved January 21, 2023, from https://www.nes-ips.com/what-are-the-benefits-of-inflatable-seals/

Nick Stewart. (2008). *Submarine escape and rescue: a brief history. Seapower center. Australia*

Ocean Grazer BV. (2022). Utility Scale Offshore Energy Storage. Ocean Grazer.
https://oceangrazer.com/

Persson B. N. J., Albohr O., Tartaglino, U., Volokitin A. I. and Tosatti E., J.(2005) Phys.: Condens. Matter, 17 R1.

Persson, B.N.J. (2022) Fluid Leakage in Static Rubber Seals. *Tribol Lett* 70, 31.

Przemysław Jaszak, Janusz Skrzypacz, Andrzej Borawski and Rafał Grzejda. 2022. Methodology of Leakage Prediction in Gasketed Flange Joints at Pipeline Deformations. Faculty of Mechanical and Power Engineering, Wroclaw University of Science Technology,27 Wybrzeze Stanislawa Wyspianskiego Str., 50-370 Wroclaw, Poland;

Przemyslaw Lutkiewicz, David Robertson and Michael Pulvino. 2019. ESTABLISHMENT OF INDUSTRY STANDARD FLANGE SEALING EFFECTIVENESS MEASURE (LEAKAGE RATE BASED) METHODOLOGY. Proceedings of the ASME 2019 Pressure Vessels & Piping Conference PVP2019

Qiang Zhang, Xiaoqian Chen, Yiyong Huang and Xiang Zhang. 2018. An Experimental Study of the Leakage Mechanism in Static Seals. college of Aerospace Science and Engineering, National University of Defense Technology, Changsha 410072, China; chenxiaoqian75@126.com (X.C.); zxstudy@hotmail.com (X.Z.)

Richard S., (2021), LR11 submarine rescue vehicle to ship for Indo-Pacific navy. Janes news.https://www.janes.com/defence-news/news-detail/lr11-submarine-rescue-vehicle-to-ship-for-indo-pacific-navy (accessed at 26-10-2022)

Robert Flitney. 2015. Seals and Sealing Handbook sixth edition. IChemE Advancing chemical engineering worldwide

Rutkowska, M., Heimowska, A., Krasowska, K., and Janik, H. (2002). Biodegradability of polyethylene starch blends in sea water. Polish Journal of Environmental Studies, 11.

S.Lassesen, T.Erikson, F.Teller,. 2002. “NORSOK L-005; Compact Flanged Connections (CFC) – The New Flange Standard”, ASME PVP 2002-1097.

Schultz MP. (2004) Frictional resistance of antifouling coating systems. J Fluids Eng 126:1039 – 1047.

Stephan G. Bullard, Sandra E. Shumway & Christopher V. Davis (2010) The use of aeration as a simple and environmentally sound means to prevent biofouling, Biofouling,

Vinagre, P. A., Simas, T., Cruz, E., Pinori, E., and Svenson, J. (2020). Marine biofouling: A european database for the marine renewable energy sector. Journal of Marine Science and Engineering, 8(7):495. PT: J; TC: 8; UT: WOS:000556382400001.

V V Kostenko *et al.* 2019. Underwater Robotics Complex for Inspection and Laser Cleaning of Ships from Biofouling. *IOP Conf. Ser.: Earth Environ. Sci.* **272** 022103

V. Zheden, W. Klepal, S. Gorb and K. A, (2015).“Mechanical properties of the cement of the stalked barnacle Dosima Fasiculari,” *Royal Society Publishing,* vol. 5, no. Interface Focus, pp. 1-9.

Weinell CE, Olsen KN, Christoffersen MW, Kiil S. (2003) Experimental study of drag resistance using a laboratory scale rotary set-up. Biofouling 19(Suppl.):45 – 51.

Appendices

A: Gantt chart

Designing a Diving bell

Ocean Grazer

Activity\week	1	2	3	4	5	6	7	8	9	10	11	12
Designing reserach	RDP											
Literature research												
Feedback												
Gathering and designing experiment												
Doing the experiment												
Reporting results												
Feedback												
Intermediate report							14/12					
Redesign and replicating experiment												
Final reporting												
preliminary report											10/01	
Final version												20/01

B: Seals

Figure .1 and .2: Seal A

Outer diameter = 7,2 cm
Inner diameter = 4,6 cm
Thickness = 0,35 cm
Area = 24,09 cm^2
Young's elastic modulus=?

Figure .3 and .4: Seal B
Outer diameter = 6,22 cm
Inner diameter = 4,2 cm
Thickness = 0,22 cm
Area = 16,53 cm^2
Young's elastic modulus=?

Figure .5: Seal D
Outer diameter = 8,38 cm
Inner diameter = 4,38 cm
Thickness = 0,23 cm
Area = 40,09 cm^2
Young's elastic modulus=?

C: Flange

Flange:

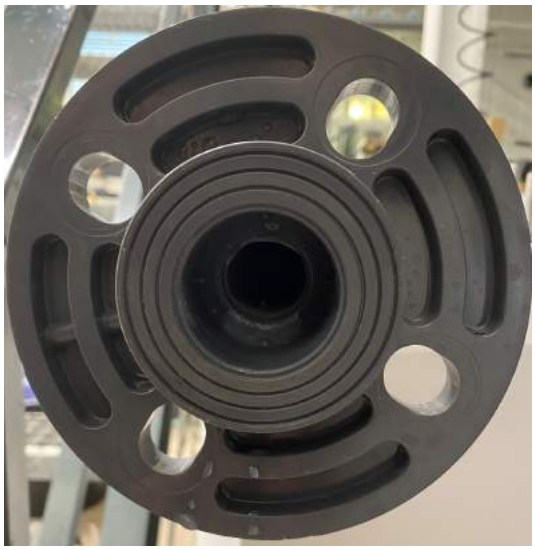

Figure .6 and .7: bottom view of flange in .7 and side view of the flange connection in .8
Inner diameter= 4 cm
Outer diameter= 7,28cm
area = 29,05 cm^2

D: Scans of sandpaper

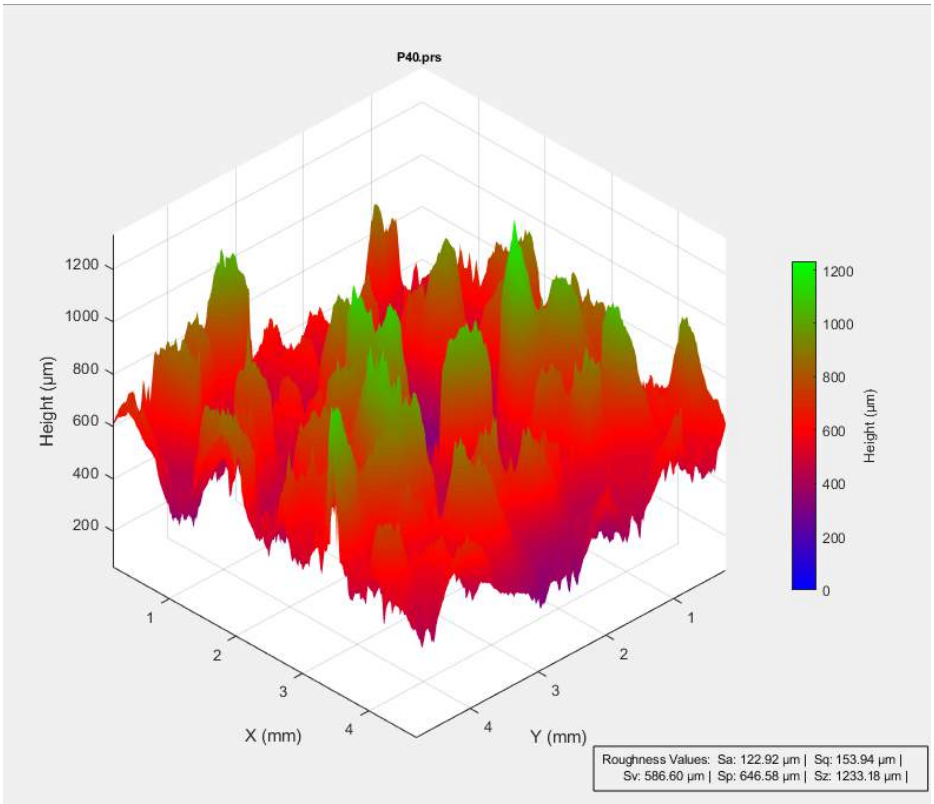

Figure .8: Scan of P40 sandpaper with a roughness of 122,92 Ra

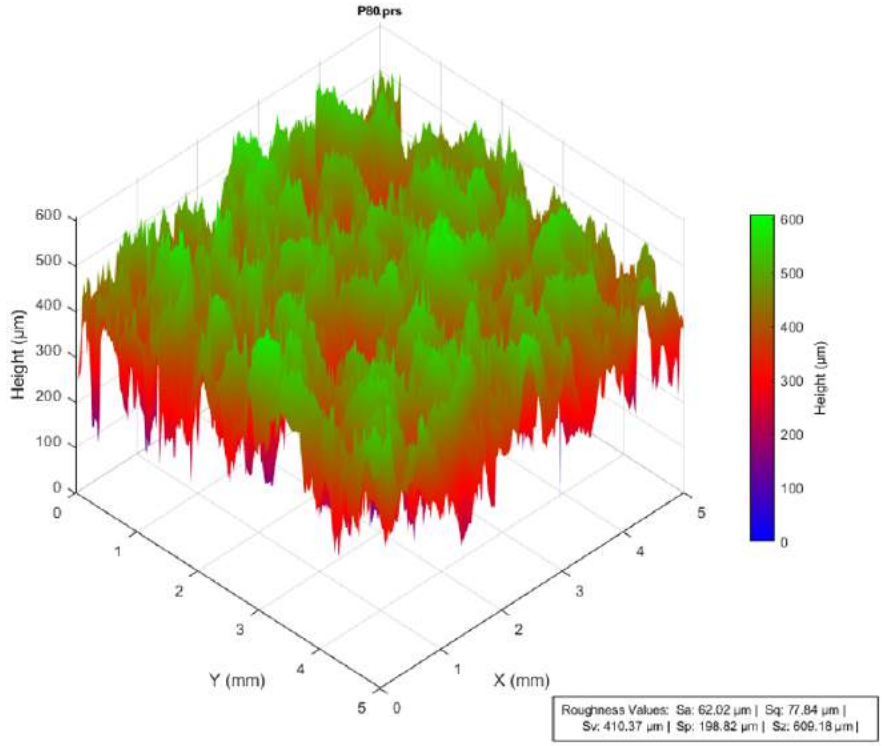

Figure .9: Scan of P80 sandpaper with a roughness of 62,02 Ra

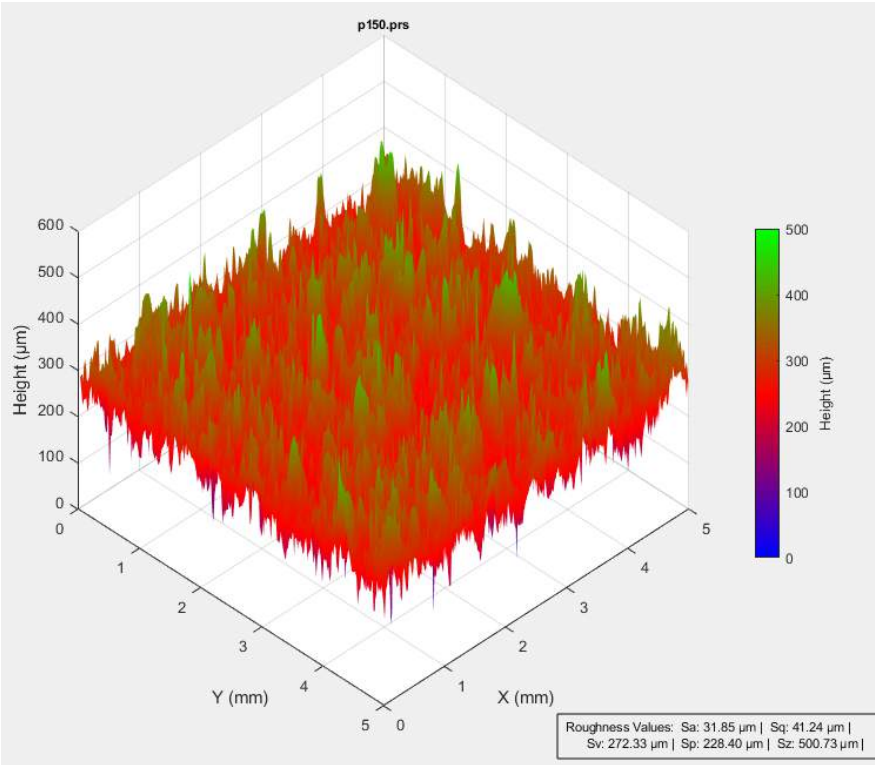

Figure .10: Scan of P150 sandpaper with a roughness of 31,85 Ra

E: Torque wrench

Figure .11: Torque wrench

F: 3D optical profilometer

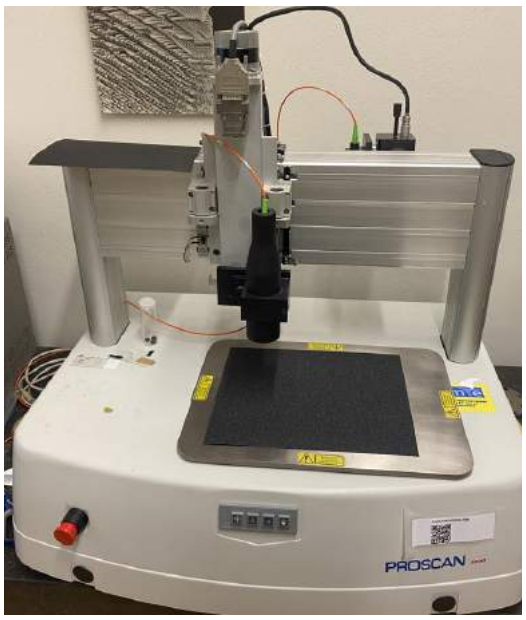

Figure .12: 3D optical profilometer used at the UMCG

G: Roughness steel

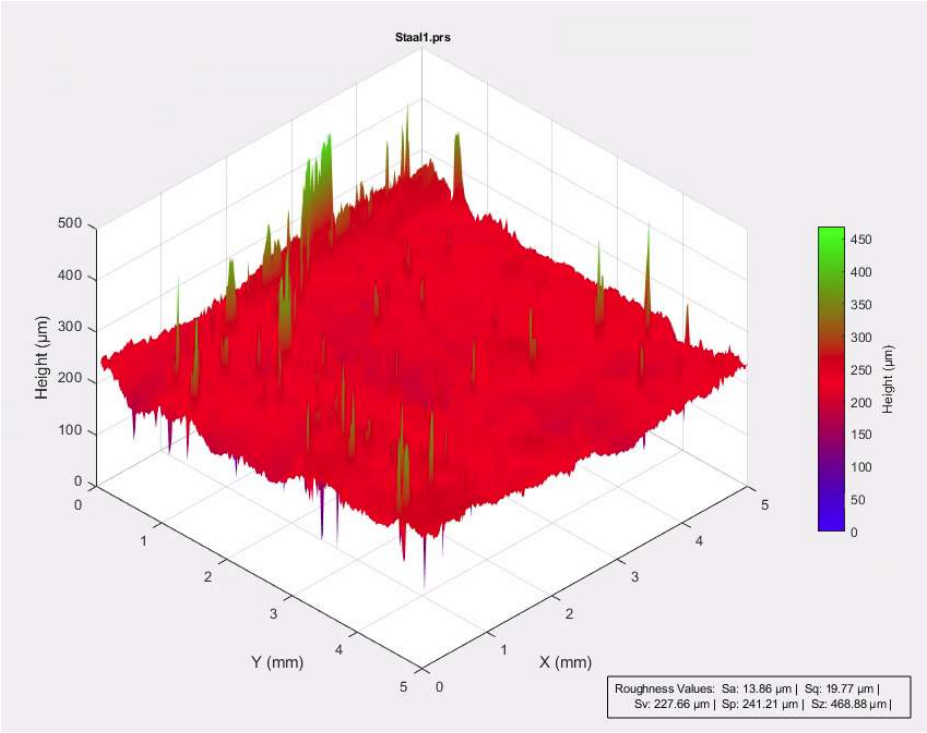

Figure .13: Surface roughness of cleaned steel surface. Showing a surface roughness of 13,86 Ra

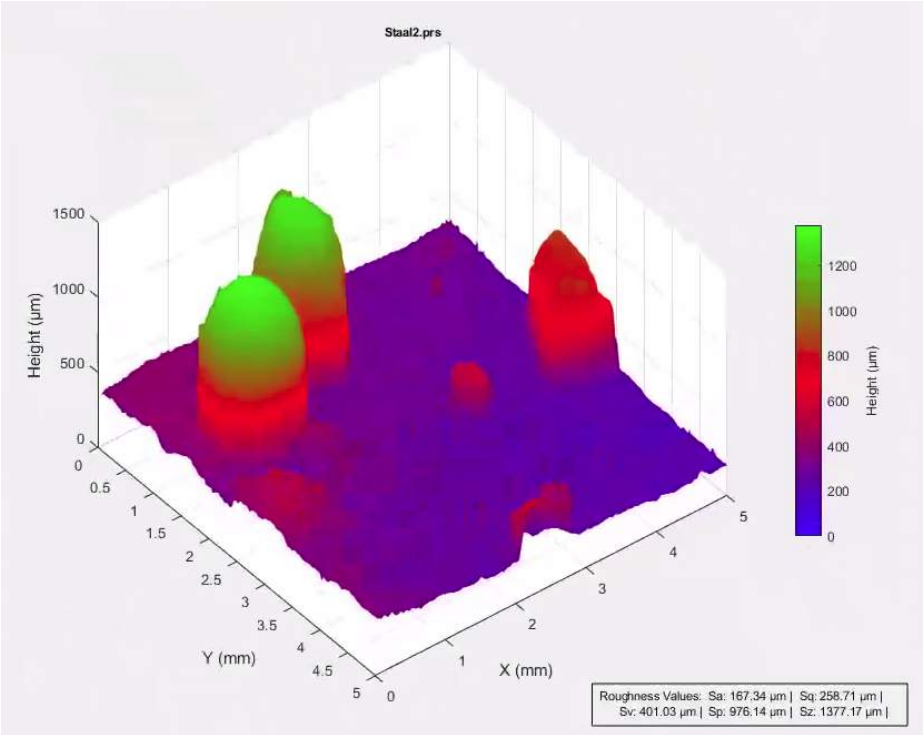

Figure .14: Surface roughness of cleaned steel surface with some remaining sand. Showing a surface roughness of 167,34 Ra

H: Plastic deformation seals

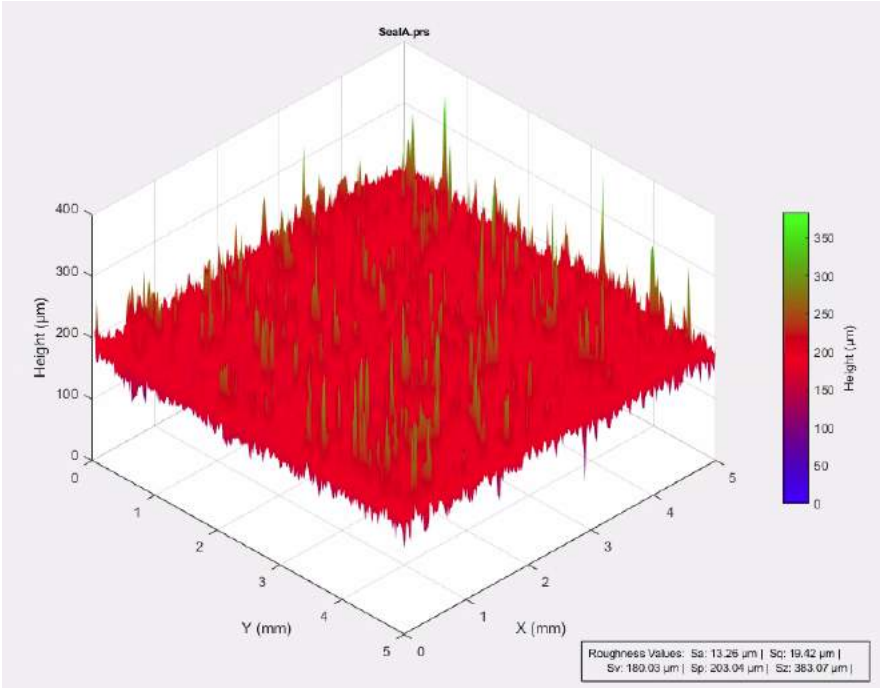

Figure .15: Surface roughness of the plastic deformation of seal A. Showing a surface roughness of 13,26 Ra

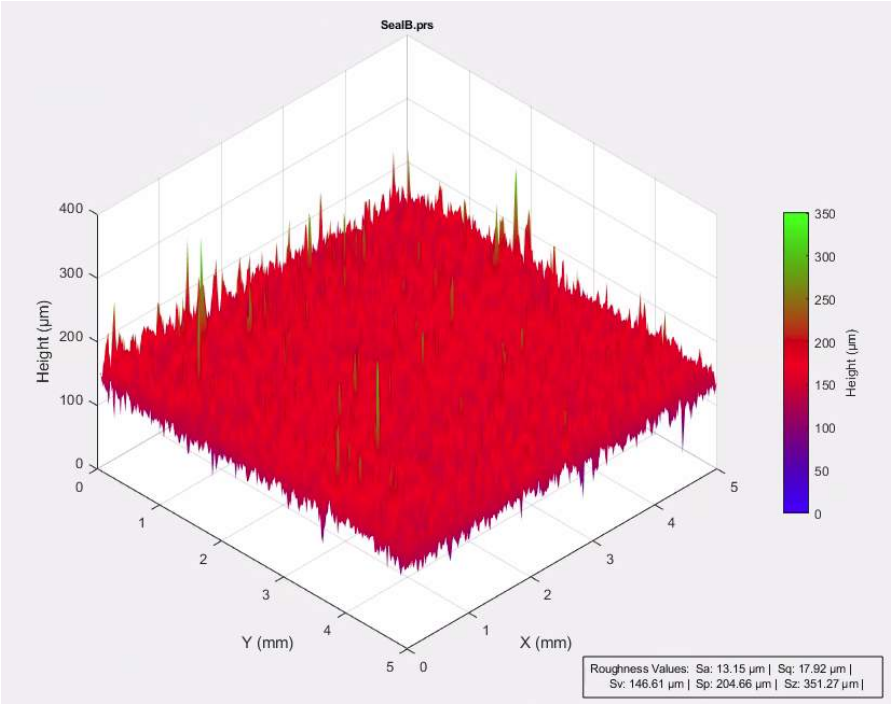

Figure .15: Surface roughness of the plastic deformation of seal A. Showing a surface roughness of 13,15 Ra

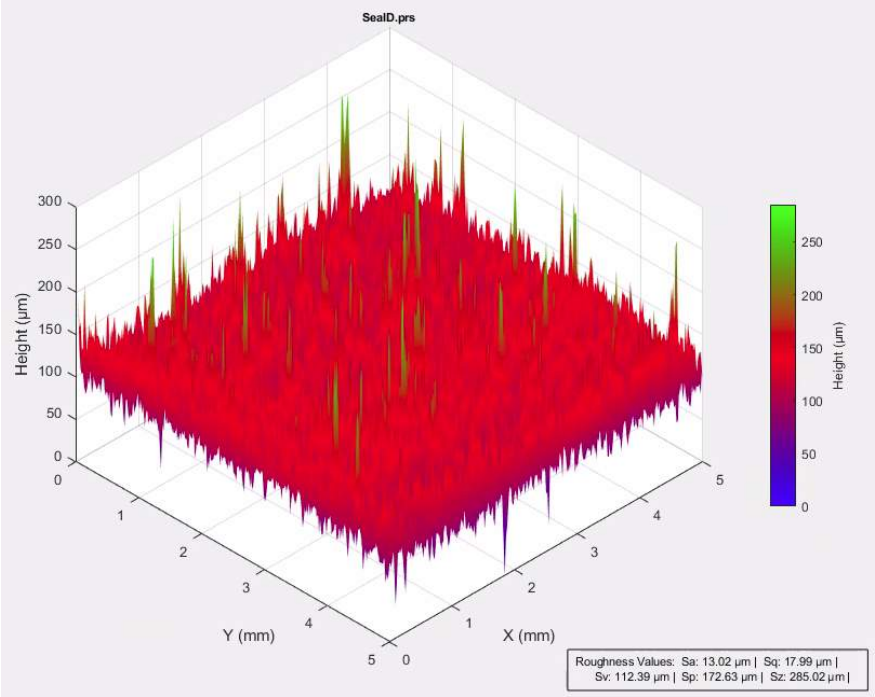

Figure .16: Surface roughness of the plastic deformation of seal A. Showing a surface roughness of 13,02 Ra

I: Blind flange

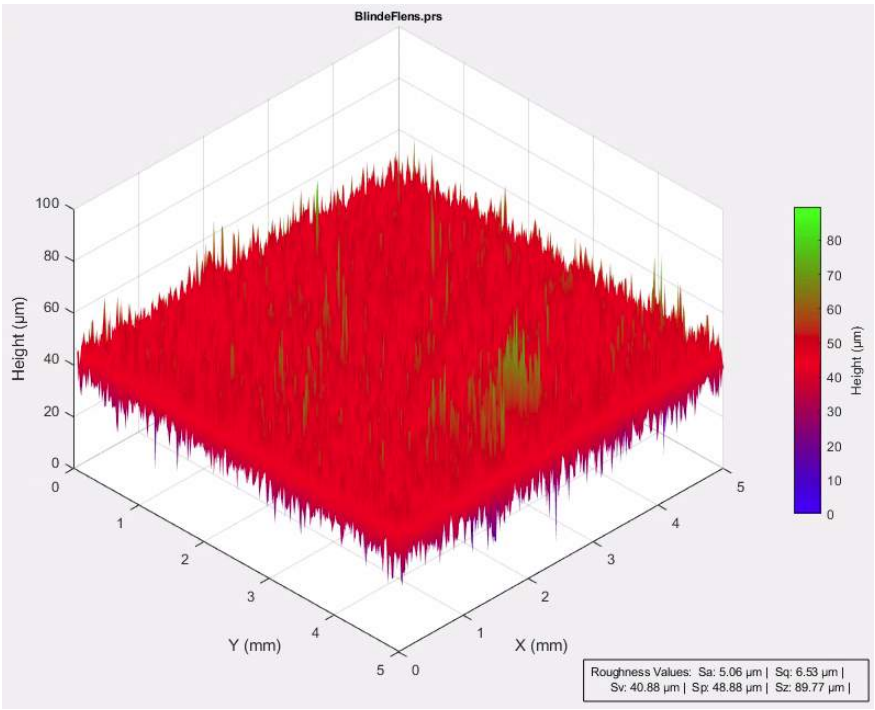

Figure .17: The surface roughness of the blind seal is 5,06 Ra.

J: Cleaned Steel

Figure .18: Collected piece of steel